Title	
Author(s)	Srihakulung, Ornin
Citation	
Issue Date	2018-09
Type	Thesis or Dissertation
Text version	ETD
URL	http://hdl.handle.net/10119/15527
Rights	
Description	Supervisor:　　　　　, 　　　　　　,

Molecular Interactions in
Inclusion of Complexes with Cyclodextrins

Ornin Srihakulung

Japan Advanced Institute of Science and Technology

Doctoral Dissertation

Molecular Interactions in
Inclusion of Complexes with Cyclodextrins

Ornin Srihakulung

Supervisor: Prof. Ryo Maezono, Ph.D.

School of Information Science
Japan Advanced Institute of Science and Technology

September 2018

MOLECULAR INTERACTIONS IN INCLUSION OF COMPLEXES WITH CYCLODEXTRINS

A Dissertation Presented

By

ORNIN SRIHAKULUNG

1520205

Submitted to

School of Information Science

Japan Advanced Institute of Science and Technology

In partial fulfillment of the requirement for the degree of

DOCTOR OF PHILOSOPHY

Approved as to style and content by

Supervisor: Prof. Ryo Maezono, Ph.D.

Second Supervisor: Prof. Hiroyuki Iida, Ph.D.

Committee Members: Prof. Satoshi Tojo, Ph.D.

                     Assoc Prof. Kenta Hongo, Ph.D.

External Examiner: Assoc Prof. Dam Hieu Chi, Ph.D.

                     Prof. Tamio Oguchi, Ph.D.

                     Assoc Prof. Luckhana Lawtrakul, Ph.D.

SEPTEMBER 2018

Abstract

MOLECULAR INTERACTIONS IN INCLUSION OF COMPLEXES WITH CYCLODEXTRINS

by

Ornin Srihakulung

Bachelor of Industrial Engineering, Chiangmai University, 2006

Master of Metallurgy Engineering, Chulalongkorn University, 2014

Most case studies of Thai traditional drugs (herbal products) have shown a similar problem of the substance degradation that can cause the instability in the active compounds, including Plumbagin. Basically, encapsulation technique is adopted to address this problem and widely employed to improve the stability of numerous compounds in diverse industries. Binding energy is an important value in the inter-molecular interaction between host and guest molecules, that can directly affect the drug efficiency from the release of active compound to the target cell. *Ab initio* investigation of the binding energy is an important tool to provide useful theoretical predictions. Density Functional Theory (DFT) is most suited to do this. However, its dependence on the exchange-correlation (XC) functionals means that it is necessary to assess the strengths and weaknesses of these functionals for the relevant system. This is the main objective of this study.

To consider the molecular and organic system, B3LYP functional is generally viewed as the most suitable XC functional. However, it is unable to properly account for inter-molecular interaction, of which dispersion forces (and therefore, dispersion-corrected functionals) is a vital part. A total of five dispersion-corrected functionals were assessed in this study: CAM-B3LYP, B3LYP-GD3, CAM-B3LYP-GD3, M06-2X, and M06-2X-GD3. The conventional hybrid DFT (B3LYP) provides positive binding energy, which means it cannot capture the dispersion force from an inter-molecular interaction. Dispersion correction functionals, meanwhile, give negative values of binding energy, with DFT-GD3 providing the precise and lowest binding energies. These *ab initio* results are compared also with those

of semi-empirical methods. Of these, the PM7 method presents the lowest binding energy, though we observe significant overestimations.

Keywords: Cyclodextrins, Encapsulation, Inclusion complex, DFT, Dispersion functional

Acknowledgments

Table of Contents

This dissertation was prepared according to the curriculum for the Collaborative Education Program organized by Japan Advanced Institute of Science and Technology and Sirindhorn International Institute of Technology.

List of Figures

List of Tables

List of Abbreviations

ACD/αCD	α-Cyclodextrin
ACFDT	Adiabatic-Connection Fluctuation-Dissipation Theorem
B88	Becke 1988
BCD/βCD	β-Cyclodextrin
BSSE	Basis Set Superposition Error
B3LYP	Becke, 3-parameter, Lee-Yang-Parr
CAM-B3LYP	Coulomb-attenuating method-Becke, 3-parameter, Lee-Yang-Parr
CBS	Complete Basis Set
CDs	Cyclodextrins
CP	Counterpoise Corrections
DFT	Density Functional Theory
GCD/γCD	γ-Cyclodextrin
HF	Hartree-Fock
HF-SCF	Hartree-Fock Self- Consistent Field
HPBCD	Hydroxyl Propyl-β-Cyclodextrin
HOF	Heats of Formation
HOMO-LUMO	Highest occupied molecular orbital - Lowest unoccupied molecular orbital
LC	Long-range-corrected
LCAO	Linear Combination of Atomic Orbitals
LPS	Lipopolysaccharide
MBCD	Methyl-β-Cyclodextrin
NCI	The National Cancer Institute
NDDO	Neglect of Diatomic Differential Overlap
NDO	Neglect of differential overlap
PB	Plumbagin
PM3	Parameterization Method 3
PM6	Parameterization Method 6
PM7	Parameterization Method 7
SCF	Self-Consistent Field
UEG	Uniform electron gas
vdW	van der Waals
vdW-DF	van der Waals density functional

Chapter 1

Introduction

1.1 Motivation

Thai herbs are excellent examples of economically important plants, which can be distributed in all kinds of high quality and usable products for the market, from pharmaceuticals, cosmetics, to food production. These products are related to challenging issues such as the compound instability, lack of aromatic permanence (e.g. perfumes), and other issues related to chemical and physical properties of the products. An important issue is that of the preservation of these products, which can lead complications in the production line and increase the cost of the product. Additionally, the use of herb products is required in a very large quantity, since there is no transformation or extraction of the active compound to be used directly. Usage of Thai herbs involve a greater amounts of herbs and frequency to get equally desired effects as Chinese herbs and other traditional medicines. As a result, the packaging of Thai herb products is usually larger in quantity and volume, which can inflate the transportation costs and the shelf space in the logistic system. In addition, there are difficulties and complications in its usage, which requires a novel technology to address these problems more efficiently. Some expensive rare herbs or active compounds such as Sandalwood, Agarwood, and off-season plants usually suffer from product shortage. In addition, they are unable to maintain a good condition due to the deterioration from air and sunlight, which can diminish the price and quality of these substances.

Consequently, the use of the highly effective and affordable technique of nanoencapsulation is recommended to prolong the period of compound retention and to provide protection from sunlight and humidity. Moreover, this technique can efficiently decrease the amount of herb used in the initial product, thus reducing the cost and increasing the value of herbal products. In the nanoencapsulation scheme, a 'guest' molecule is encapsulated or inserted inside a 'host' molecule, which protects it from harmful external factors. The inter-molecular interaction between 'guest' and 'host' is the key, since it determines much about the resulting 'host-guest inclusion complex'. A primary predictor in this mechanism is the binding energy, the existing potential energy between these molecules. It can be directly translated into how easily these complexes form when 'guest' and 'host' molecules interact with one

another, as well as how difficult it will be to coax the 'host' molecule to release the 'guest' when, for example, drugs need to be delivered to the target system.

A reliable theoretical prediction for the binding energy may be obtained using *ab initio* methods. Density Functional Theory (DFT) is a well-known *ab initio* method widely utilized to tackle such problems. However, the predictions of DFT is strongly related to the choice of exchange-correlation (XC) functional used in the calculation. The choice of XC functionals is an integral decision for researchers, made with respect to the quantum system investigated. There has been little usage of DFT in evaluating host-guest inclusion complexes, which presents an issue as to the appropriate choice of XC functional. An assessment of available XC functionals is helpful to better inform future studies in this matter. This work aims to provide such an assessment.

As inter-molecular interaction is most important in predicting the binding energy, XC functionals which properly account for dispersion forces (dispersion-corrected functionals) are likely appropriate choices. We investigate a conventional hybrid XC functional (B3LYP) as well as dispersion-corrected functionals for a system of host-guest inclusion complex. Calibration is also made with results from semi-empirical methods: PM3, PM6, and PM7. We take plumbagin (the active compound in Benjakul) as the guest molecule, and encapsulate it with cyclodextrins (host molecules). Calculation results may reveal pertinent information relating to the qualities of each XC functional, to better set a foundation for future endeavors.

1.2 Problem Statement

The main problem of this work is the instability of the active compounds or plumbagin in Benjakul. The compounds in Thai medicinal plants easily sublimate and loss their properties. Plumbagin is unstable and very reactive with sunlight and sensitive to temperature. Therefore, we have to keep it under low temperature ($-20°C$), because of the low melting point of plumbagin at $76-78°C$. As a result, those conditions increase the complexity and cost of the production process to preserve the anti-cancer activity of these compounds.

1.3 Objective and Scope

In this study, binding energies of several model host-guest inclusion complexes are calculated by DFT with different choices of XC functionals. Plumbagin is chosen as the model guest molecule, while β-cyclodextrin (BCD) and its derivatives, Methyl-β- Cyclodextrin (MBCD) and Hydroxyl Propyl-β-Cyclodextrin (HPBCD), are used as model host molecules. The model host-guest inclusion complexes are taken to reside in a vacuum environment. The XC functionals investigated in this work include the conventional hybrid functional B3LYP

and dispersion-corrected functionals: CAM-B3LYP, M06-2X, B3LYP-GD3, M06-2X-GD3, and CAM-B3LYP-GD3. The results are calibrated with other results from semi-empirical methods: PM3, PM6, PM7, which will provide a point of comparison to determine a measure of reliability for the calculated values. Therefore, this research aims to clarify the appropriateness, weaknesses, and limitations of each choice of XC functional.

1.4   Our Contributions

The geometry orientation of the guest molecule with respect to the host is a challenging aspect of this study. This obstacle naturally arises for systems with a low degree of symmetry. Inorganic crystal structures and a few simple organic molecules (e.g. benzene rings) generally do not present this issue, while the opposite is true for most organic molecules, such as those investigated in this study [14]. Innumerable possibilities exist for the geometry of the host-guest complex, and the optimization of such structures are much too expensive for *ab initio* methods. Ideally, a few candidate conformations needs to be selected from all the possible host-guest geometry configurations, while keeping a reasonable computational cost. This selection process is the most challenging part in this work. Our approach is to employ a semi-empirical evaluation of the possible geometries by running docking calculations. The Lamarckian genetic algorithm is utilized in order to find the ideal candidate conformations. The host molecule is considered fixed in a vacuum, while the guest molecule is allowed to have a free range of movement. 100 movements of the guest molecule are performed. The final geometries are collated and classified into groups of possible conformations, each with calculated values of binding energy and 'frequency of occurence. These values are the basis of selecting appropriate candidate conformations considered for *ab initio* calculations. From the results, we extract two possible conformations,'up' and 'down', based on the geometry orientation of the methyl group in plumbagin with respect to the wider rim of the fixed host molecules (as illustrated in Figure 4.3). With the three types of host molecules considered in this study, a total of 6 structures are selected for the *ab initio* calculations.

We have found that, the structures which calculated from the functional with DFT-GD3 calculation provide the precise and lower binding energy. For the semi-empirical calculation, PM7 provide the lowest binding energy, but the result is overestimated as shown in the previous studied, which expressed PM7 is good for only the small system. But it cannot describe the interaction in the large system [13] as our system. In conclusion, we found the most suitable functional which can express the weak intermolecular between two molecules and also found the suitable inclusion complex which is DFT-GD3.

1.5   Thesis Structure

This thesis contains five chapters, where the Chapter 1 gives an introduction of the research. In addition, the problem statement, objective and scope, proposed approaches, and the contributions are included in this chapter. In Chapter 2, the background and related works on host and guest molecules, and the interaction between them are illustrated. The theoretical framework, such as the semi-empirical and *ab initio* method, including the computational procedure are provided in Chapter 3. In Chapter 4, results and discussions are presented. Finally, Chapter 5 includes the conclusion and the recommendations for future studies.

1.6   Computer Software

All of the semi-empirical and DFT calculation described in this dissertation were carried out using Gaussian09 [15] program. GaussView5.0 [16] program package is used for final structural observation and constructing small molecule, electronic structure and energies of atoms, molecules, and surfaces which can produce various results using semi-empirical and *ab initio* method. The program can be used to investigate various systems by deploying Gaussian09, including inorganic or organic molecules. With Gaussian09, it can be used to predict the structures, binding energies, reactions and thermodynamic properties.

1.7   Units

Most of the calculation results are in kilocalorie per mole (kcal/mol), in which the author has stated beforehand. Otherwise, hartree atomic units (a.u.) will be conversed by 1 hartree of 627.509 kcal/mol. Please see the conversion factors between hartree atomic units (a.u.) and other units in Appendix A.

Chapter 2

Target systems

From our previous researches [17], we are interested in the active compound or plumbagin (Guest). We aim to find the suitable host to preserve this active compound in nanocapsule or cyclodextrin (Host). We studied the β-cyclodextrin (BCD) and its derivatives which are widely used in many industrials, especially pharmaceuticals. In this chapter, we elaborate the literature review of the previous related works about our target systems, as well as the interaction between them. We will focus on the properties of the electrostatic force affecting two compounds to bind together and to form the inclusion complex.

2.1 Guest molecule

Our guest molecule is plumbagin, which is one of the active compound of Benjakul. Benjakul is a Thai traditional formula being used in many applications including: health balancing and adaptogen drug for cancer patients. It consists of five traditional herbs, including fruit of *Piperchaba*, root of *Pipersamentosum*, stem of *Piperinteruptum*, rhizome of *Zingiber officinale*, and root of *Plumbago* in the same weigh ratio as shown in Figure 2.1. Folk doctors use this traditional recipes as an adaptogenic to balance body element in patients [18]. Benjakul also applied for cancer patients in order to provide the body balance

Figure 2.1: Benjakul, a Thai traditional plant preparation from Piper chaba Linn., Zingiber officinale Roscoe or ginger., Plumbaga indica Linn., Piper interruptum Opiz., Piper interruptum Opiz., and Piper samentosum Roxb, photos are taken from literature [1].

and improve the immunity before the chemotherapy [19]. It also contains anti-inflammatory by inhibiting the cytokine releasing in an inflammatory process induced by LPS in vitro study [1]. Five plant ingredients were collected and dried at $50°C$ in oven. Next, the ethanolic extraction process began with mixing 100 g of each dried-plants component. After that, we ground the plants into rough powder, then macerated with 95% ethanol. This solution was filtrated and concentrated under the reduced-pressure condition. The extract compound was kept at $-20°C$ until start the experiments [1]. From the criteria by the National Cancer Institute guidelines (NCI) , the cytotoxic activity of extracts and pure substant with IC50 values $< 30 \, \mu$g/ml and $< 4 \, \mu$g/ml. Plumbagin is an active compounds, which can provide the best cytotoxic activity against lung cancer [18]. The active compound molecule is shown in Figure 2.2.

2.1.1 Plumbagin

The notation of plumbagin rooted from the plant Plumbago [20], while its molecule is from *Nepenthes* and *Genera − Drosera*, carnivorous plant [21]. Plumbagin is an organic compound with the chemical formula of $C_{11}H_8O_3$ or (5-hydroxy-2-methyl-1,4-napthoquinone) with the potentials of neuroprotective [22], and inhabit ectopic growth [23], such as anti-breast cancer [23] and anti-lung cancer [24].
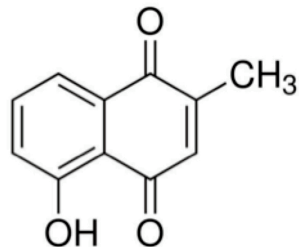
Figure 2.2: Plumbagin molecule.

Plumbagin structure consists napthoquinone, which contains two oxygen atom at 1-4 position. One methyl group substitution at 2 positions and one Hydroxyl group substitutes at position 5. Generally, there is one problem with both active compounds, especially in plumbagin which is the instability related to their low melting point (76-78$°C$) [2]. The previous study [2] illustrated the degradation of two active compounds as shown in Figure 2.3. From this figure, plumbagin degrades from 100% to 28.70% within 2 months. On the other hand, piperine sublimates only 5% during the same period of time. The degradation of plumbagin is the main problem that we are focusing in this study. The issue from instability of active compounds can be resolved by encapsulation technique similar to other compounds in the pharmaceutical industry. This technique has normally been used for protecting the ingredients and controlling active compound's releasing rate. The protection has also used to prevent the degradation from the light and oxygen or retard evaporation [25].

Table 2.1: Properties of plumbagin.

Properties	Plumbagin
Molecular formula	$C_{11}H_8O_3$
Molecular weight	188.18
Density (g/cm^3)	1.354
Melting point ($^{\circ}C$)	76-78
Boiling point ($^{\circ}C$)	383.9
Solvent solubility	Soluble in alcohol, acetone, benzene, acetic acid and slightly soluble in hot water
Stability	Stable in closed place under dry and well ventilated, but incompatible with strong oxidizing agents

Commonly, there are several types of the encapsulations. Cyclodextrin is one of the technique that can be used for the encapsulation of the drug that contains hydrophobic properties and the drug delivery through aqueous diffusion-controlled barriers [26]. Therefore, cyclodextrin is one of the technique to effectively prevent the degradation or sublimation of the compounds.

2.2 Host molecules

Cyclodextrins, discovered over a century [27], are the production of the starch interacted with an enzyme and can be used as the pharmaceutical excipients and complexing agents which can improve the aqueous solubility, stability and bio-availability or the active compound. Cyclodextrins is a natural cyclic oligosaccharide, that recently accessible as pharmaceutical excipients. Many commercialized drugs nowadays are presented in Table 2.2 [28].

2.2.1 Molecular structure

Cyclodextrins are made from natural products that constructed by digestable cellulose. The cyclic oligosaccharide consists of $(\alpha - 1, 4)$-linked α-D-glucopyranose. The center of the cavity in cyclodextrins has lipophilic properties and hydrophilic at outer surface of the structure. Chair conformation of glucopyranose holds together with oxygen, and their orientation structure like cone as shown in Figure 2.4. The $\alpha-$, $\beta-$ and γ-cyclodextrin compose 6, 7 and 8 glucopyranose units [29]. Glucopyranoses are in chair conformation, which can affect the cyclodextrins' shape likes a truncated cone rather than the cylinders. The primary hydroxyl groups position are at the narrow edge (C6), on the other hand the secondary hydroxyl groups (C2) and (C3) are at the wider rim of the cone. The apolar C3 and C5 hydrogens and ether-like are inside of the cone which can cause the central cavity to contain a lipophilic

Table 2.2: Pharmaceutical products containing cyclodextrins, data is taken from literature [11].

Drug/Cyclodextrin	Trade Name	Formulation	Company/Country
PGE_2/βCD	Prostarmon E	Sublingual tablet	Ono, Japan
PGE_1/αCD	Prostavastin	i.v. solutions and infusions	Ono, Japan Schwarz, Germany, USA
OP-1206/αCD	Opalmon	Tablet	Ono, Japan
Piroxicam/βCD	Brexin, Flogene Cicladon	Tablet Suppository Liquid	Chiesi, Italy several European countries Ache, Brasil
Benexate HCl/βCD	Ulgut Lonmiel	Capsule	Teikoku, Japan Shionogi, Japan
Iodine/βCD	Mena-Gargle	Solution	Kyushin, Japan
Dexamethasone/βCD	Glymesason	Ointment	Fujinaga, Japan
Nitroglycerin/βCD	Nitropen	Sublingual tablet	Nihon Kayaku, Japan
Cefotiam-hexetil/ αCD	Pansporin T	Tablet	Takeda, Japan
Cephalosporin (ME 1207)/βCD	Meiact	Tablet	Meiji Seika, Japan
Tiaprofenic acid/βCD	Surgamyl	Tablet	Roussel-Maestrelli, Italy
Diphenhydramin, Chlortheophyllin/βCD	Stada-Travel	Chewing tablet	Stada, Germany
Chlordiazepoxide/βCD	Transillium	Tablet	Gador, Argentina
Hydrocortisone/HPβCD	Dexocort	Solution	Actavis, Iceland
Itraconazole/HPβCD	Sporanox	Oral and i.v. olutions	Janssen, Belgium and USA
Cisapride /HPβCD	Propulsid	Suppository	Janssen, Belgium
Nimesulide/βCD	Nimedex	Tablets	Novartis and others, Europe
Alprostadil/αCD	Rigidur	i.v. solution	Ferring, Denmark
Nicotine/βCD	Nicorette	Sublingual tablets	Pharmacia, Sweden
Chloramphenicol/MβCD	Clorocil	Eye drop solution	Oftalder, Portugal
Diclofenac-Na/HPγCD	Voltaren	Eye drop solution	Novartis, France
17β -Estradiol/RMβCD	Aerodiol	Nasal Spray	Servier, France
Indomethacin/HPβCD	Indocid	Eye drop solution	Chauvin, France
Omeprazol/βCD	Omebeta	Tablet	Betafarm, Germany
Voriconazole/SBEβCD	Vfend	i.v. solution	Pfizer, USA
Ziprasidone mesylate/ SBEβCD	Geodon, Zeldox	im solution	Pfizer, USA & Europe
Dextromethorphan/βCD	Rynathisol		Synthelabo, Italy
Cetirzine/βCD	Cetrizin		Losan Pharma, Germany
Mitomycin/HPβCD	MitoExtra Mitozytrex	i.v. infusion	Novartis, Switzerland
Tc-99 Teoboroxime/HPγCD	Cardiotec	i.v. solution	Bracco, USA
Meloxicam	Mobitil	Tablet and suppository	Medical Union Pharmaceuticals, Egypt
Aripiprazole/SBEβCD	Abilify	im solution	Bristol-Myers Squibb, USA Otsuka Pharm. Co., Japan
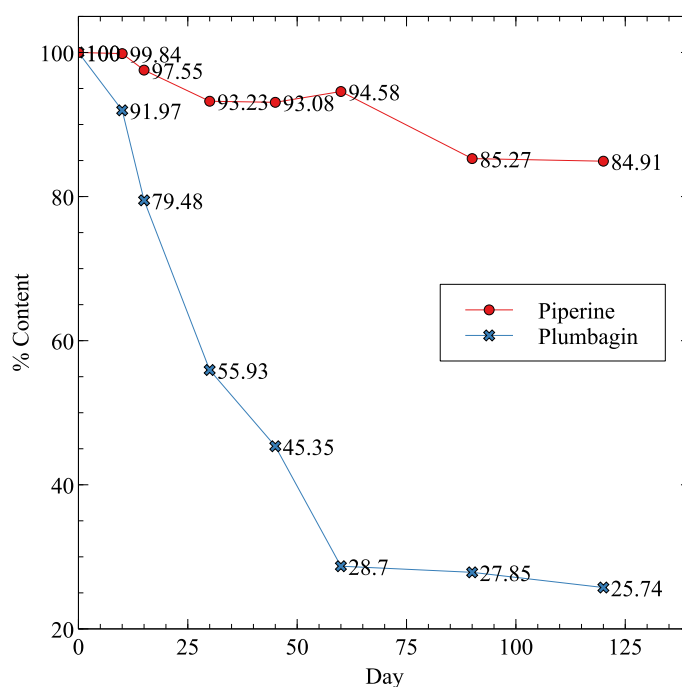
Figure 2.3: The stability test result of plumbagin and piperine in %content, the accelerated condition for testing the Benjakul ethanolic extract was set as 45+/-2°C with 75+/-3%RH, data is taken from literature [2].

property. The outside molecule shows hydrophilic character, which can dissolve in water. As the result, the cavity of cyclodextrins can form the inclusion complexes with a wide and various of guests that contain hydrophobic character. From this property, several researches and works have used this useful functionality in many applications.

2.2.2 Applications

There are several applications of cyclodextrins that can make the CDs suitable for applications in the field of analytical chemistry, pharmaceutical and food [30], such as:

- Sensitive substances (oxygen or light) stabilization;

- Substances (pigments or color) masking;

- Degradation of substances protection using micro-organisms;

- Liquid substances to powders modification;

- Chemical reactivity (guest molecules) modification;

- Volatile substances fixation;

- Ill smell and taste masking;

- Cyclodextrins with guest molecules catalytic activity.

9
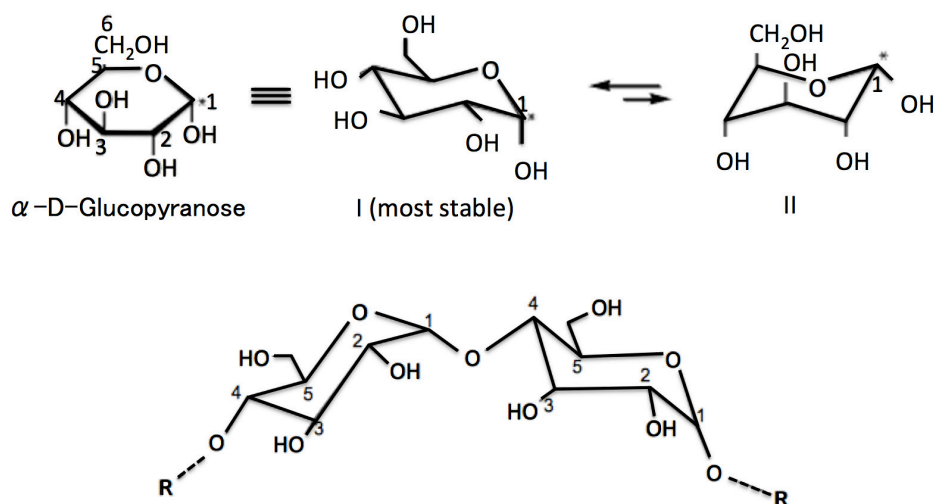
Figure 2.4: α-D-glucopyranose molecule which consists two possible types of chair conformation (I and II) and glycosidic oxygen bridge α (1,4) between two molecules of glucopyranose, figure is taken from literature [3].

2.2.3 Types

Basically, there are 3 types of cyclodextrin, which can be divided into 3 main types: α-cyclodextrin, β-cyclodextrins and γ-cyclodextrin, derived from the first generation (parent cyclodextrins). The most accessible and economical type, β-cyclodextrin, is commonly the most applicable in several industrials. On the other hand, α-cyclodextrin contains the least steric strain, while γ-cyclodextrin contains the highest strain [31]. Modifications can improve some of the properties as shown in the Table 2.3, consisting of the stability against oxygen or light, solubility, and also aids in controlling the guest molecules chemical activity. Otherwise, the cavity volume is always the first property to consider to make it proper with the host, however, it is an optional than optimal solubility and safety data [32].

Because of the 6 Å of cavity in BCD, it is suitable for accommodating for aromatic groups. Therefore, many drug molecules were encapsulated by BCD molecule. From the previous work, the molecular modeling [33] and the experimental studies [34] have shown that plumbagin molecule is normally selected to form the inclusion complex with β-cyclodextrin (BCD). Hence, this research is focusing on the inclusion complex, which are formed between plumbagin and BCDs molecules.

2.2.4 β-cyclodextrin and its derivatives

From the parent cyclodextrins, many cyclodextrins derivatives have been further synthesized. The productions of the derivatives are aminations, esterifications of primary and secondary hydroxyl groups of the cyclodextrins. The differences of groups and number of substitutions can make the properties of derivatives to change from their parents. Normally, all derivatives can change hydrophobic cavity volume. The improvement of solubility, stability
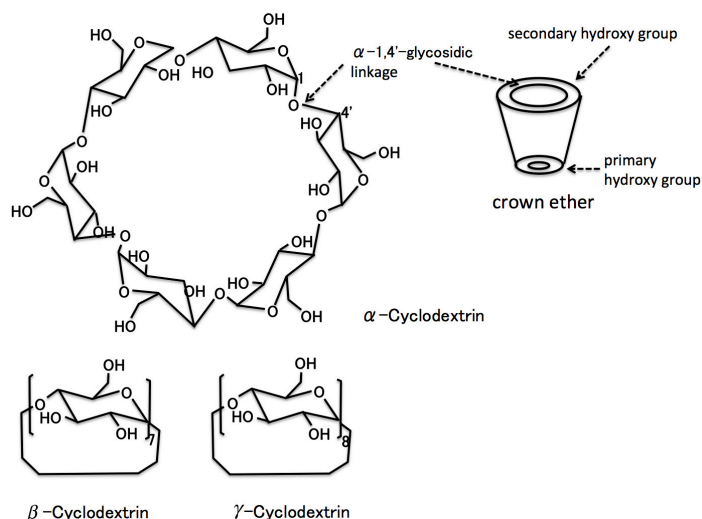
Figure 2.5: Microstructure of cyclodextrin molecules of glucopyranose. α-cyclodextrin contains 6 molecules of glucoses, β-cyclodextrin with 7 molecules and γ-cyclodextrin with 8 molecules, figure is taken from literature [4].

Table 2.3: Comparing table of the properties of each type of cyclodextrin [12].

Properties	α CD	β CD	γ CD
Molecular weight	972	1,135	1,297
Glucose monomers	6	7	8
Internal cavity diameter (Å)	4.7-5.3	6.0-6.6	7.5-8.3
Water solubility (g/100mL @T=25°C)	14.2	18.5	23.2
Melting range (°C)	255-260	255-265	240-245
Water of crystallisation	10.2	13-15	8-18
Water molecules in cavity	6	11	17
Cavity volume (ml/mol)	174	262	472
Price (US/g pharma grade)	1.0	0.025	0.8

and chemical interaction of guest molecules are gained. In this research, the BCD contains the suitable cavity size with plumbagin, however the limitation of solubility is the main problem of BCD (18.5 mg/mL). As a result, the derivatives are considered in this research with correlated two factors:

- Substitution group;

- Number of substitution.

2.3 Interaction between host and guest

The prominent point of cyclodextrins is the forming property of inclusion complex between host and guest in a wide range, even in the solid, liquid and gas phases [27]. The guest molecules are held in the cavity of cyclodextrins. The lipophilic cavity of cyclodextrins
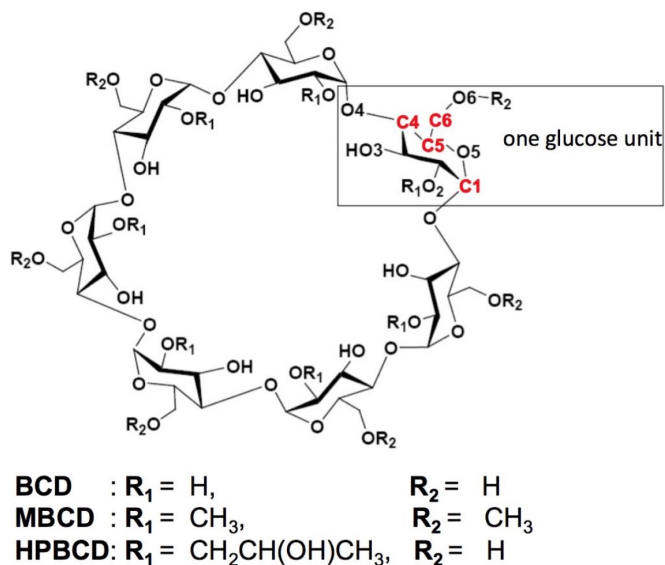
Figure 2.6: Schematic representations of BCD and its derivertives (MBCD and HPBCD), which R1 and R2 position were substituted by methyl and hydroxylpropyl-group, adapted from [5].

Table 2.4: β-cyclodextrin and its derivative properties, data is taken from literature [6].

Information	BCD	MBCD	HPBCD
Product name	Beta-cyclodextrin	Methyl-beta-cyclodextrin	Hydroxylpropyl-beta-cyclodextrin
Chemical formula	C42-H70-O35	C56-H98-O35	C45-H76-O36
CAS#	7585-39-9	128446-36-6	94035-02-6
Molecular weight	1135	1310	1454
Melting point ($^\circ C$)	260	180-182	305
Flash point ($^\circ C$)	-	187	-
Bulk Density	-	400 kf/m3	-
Price (USD/g)	0.025	111.88	7.0781

offer the proper environment to non-polar of the host to form the inclusion complex [35]. The host and guest binding is a dynamic equilibrium, and the strength of binding is related to how suitable between host and guest are, also specific local interactions of their surface atoms.

The ability of formation of the inclusion complex between cyclodextrins and guest is a function of two key factors:

1. Steric or spatial arrangement of atoms in molecules that related to size of cyclodextrins cavity and guest. For instance, if the guest's size is bigger than the host's cavity, they are unable to fit properly.

2. The thermodynamic interaction between host and guest, for favorable case, the total energy driving force is shown in negative value that will pull the guest into the cyclodextrins.
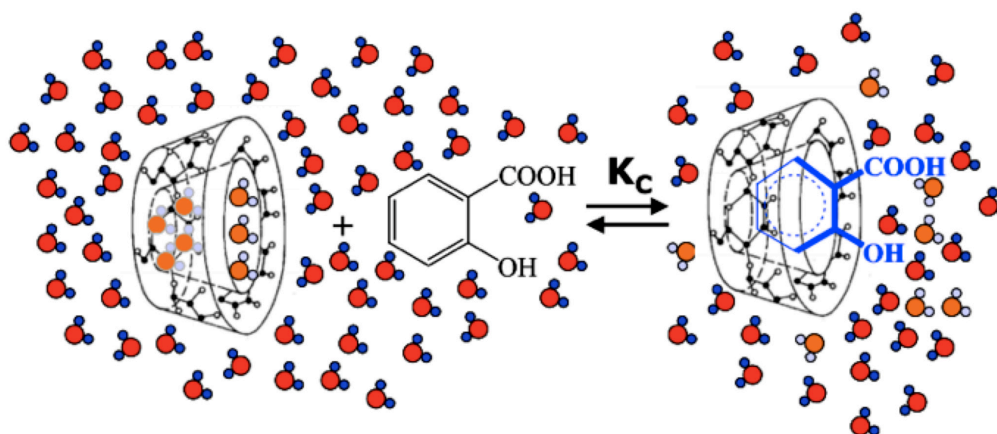
Figure 2.7: Mechanism of inclusion complex between ligand and cyclodextrin, figure is taken from literature [6].

Primarily, energetically supportive interactions consist of 4 types that can shift the equilibrium in order to form the inclusion complex:

1. Repulsive interactions decrement from the water environment and hydrophobic guest;

2. Hydrogen bonds increasing formed as displaced water depart to the larger pool;

3. Polar water molecules displacement from a non-polar cavity;

4. Hydrophobic interactions rising by inserting guest into polar CD cavity.

To form complex, the initial equilibrium is quite accelerated (in a minute), while on the other hand, the final equilibrium is time consuming to reach. Several techniques can be used to form the inclusion complexes, depending on the active compound (guest), equilibrium kinetics, processes and other ingredients. To visualize the inclusion complex, we can use the molecular modeling by computational chemistry. Table 3.3 summarizes the program and basic sets from the existing literatures.

If we consider the interaction between host and guest molecule directly, it does not related to only size and shape molecule. Since our system consists of neutral guest and host, dipole-dipole interaction plays an the important role in intermolecular interaction. The non-covalent interactions are stabilized the inclusion complex molecules. The total stabilization of a molecule usually between 1 and 20 kcal/mol, which are considered as small binding energy compared to a covalent bond energy = 100 kcal/mol. To describe non-covalent interactions, the accurate methods of quantum chemistry are required. Only semi-empirical or the conventional DFT are insufficient. The BCD inclusion complexes with others active compounds are reviewed and concluded as in Table. 2.5. The binding energies of PM3 are in the range of -33.19 to -3.36 kcal/mol. For PM6 is between -21.68 to 5.38 kcal/mol. For DFT calculation, we can group in to three parts; the basis set which consider BSSE calculation,
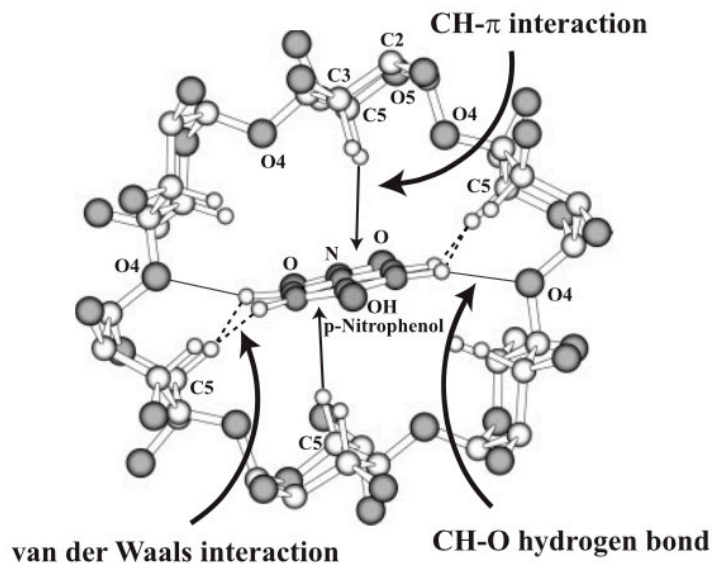
Figure 2.8: Host-guest interaction observed in α-cyclodextrin complex with p-nitrophenol, figure is taken from literature [7]

does not consider and the last one is DFT included dispersion functional calculation. The further information of the calculation method will be describe in the next chapter.

The interactions between host-guest molecules are consisted of:

1. hydrogen bond

   The hydrogen bond between host-guest molecule can be divided into two types including:

   - O-H, N-H and F-H, this type is the hydrogen bond between cyclodextrin' hydroxyl groups with guest molecule, which mostly restricted to the primary O(6)-H side. Because of the more flexible of the primary side than the secondary O(2) and O(3).

   - C-H...O hydrogen bond, this type of hydrogen bonds are weaker hydrogen bond donor than O-H, N-H and F-H. Therefore their donor potential could not be ignored (ca 2-8 kJ/mol) [44]. These bonds is importance in many organic system, because this bond is more polarized than $C(sp^3)$-H in pure hydrocarbons. The charge is +0.13 (compared to hydroxyl group is +0.34) [45]. Normally, C-H...O interaction appears between polar guest with the cavity lining of host molecules. For the calculation, the estimated energies interaction slightly above 4 kJ/mol, which is a quarter to a third of conventional hydrogen bonds.

2. Electrostatic interactions

Table 2.5: Binding energy range of the similar system which is encapsulated with β-cyclodextrin.

Method	Guest	binding energy (kcal/mol)	reference
Calculation			
1.1 semi-empirical			
1.1.1 PM3	linalool	-12.58 to -7.02	[36]
	eugenal	-9.72 to -7.57	[36]
	methyl eugenol	-13.53 to-10.09	[36]
	estragole	-7.01 to -5.39	[36]
	eugenol	-12.77	[36]
	PNBA1	-9.80 to -8.20	[37]
	PNBA2	-33.19 to -21.88	[37]
	sulfonamide	-4.45 to -3.36	[38]
	carvacrol	-25.12 to -23.09	[39]
1.1.2 PM6	tyrosine	-21.68 to -18.19	[40]
	sulfonamide	2.94 to 5.38	[38]
	Ortho-Anisidine	-13.50 to -13.20	[41]
1.1.3 PM7	tyrosine	-53.17 to -51.89	[40]
1.2 *ab initio*			
1.2.1 B3LYP/3-21G*	sulfonamide	-22.65 to 34.97	[38]
1.2.2 B3LYP/6-31G(d)	linalool	-2.46 to -0.36	[36]
correction with BSSE	eugenal	-10.55 to 0.66	[36]
	methyl eugenol	1.20 to 2.34	[36]
	estragole	-0.30 to 1.20	[36]
	eugenol	2.01	[36]
	PNBA1	-94.8 to 100.4	[37]
	PNBA2	-12.53 to 0	
	carvacrol	-11.62 to -6.07	[39]
1.2.3 M05-2x/6-31G(d)	carvacrol	-25.13 to -18.18	[39]
Experimental (Heat of formation)			
	carvacrol	-3.74	[42]
	t-cinnamaldehyde	-3.51	[43]
	Eugenol	-1.82	[43]
	Cinnamon bark extract	-4.94	[43]
	Clove bud extract	-10.28	[43]

The electrostatic includes all of the electrostatic forces such as, force between the permanent charge or between dipoles and the higher dipoles. Electrostatic interaction consists 3 important types: ion-ion, ion-dipole and dipole-dipole interaction. For cyclodextrin inclusion complex system, therefore cyclodextrin normally exists as neutral molecules. In addition, the cyclodextrin are substituted with some appropriately functionals group.

The ion-dipole interactions of cyclodextrin system normally are increase from ionic charge of guest molecule. Some guests consists of the dianions such as SO_4^{-2} or CO_3^{-2}, which can be increase binding force from the tightly bond with cyclodextrins. The dipole moments of cyclodextrin were study, the range between 10-20 D is suggested as a highly polarized [46]. For the normally the cyclodextrin complex contains small dipole moment in the range of 2-4 D, which obtain from the various theoretical methods. In the case of high dipole moment that can play in the important role in the inter molecular interaction in this system. For dipole-dipole interactions, many study about several substitution benzene derivative of guest which expresses dipole [47,48]. Their dipoles are anti parallel to host molecule. Dipole-dipole play in the important role to stabilizing the complex, and it related to the orientation of guest molecule.

3. Van der Waals interactions

Van der Waals forces or London dispersion interaction consists of the combination between induction and dispersion forces and only dispersion force. Nowadays, this force is the important evident which are responsible for many phenomena in physic, chemistry and biology. While vdW interaction is very weak force comparing to ionic, metallic and covalent bonding, but this force plays in the important role to determine the stability and structure of various compounds.

Many researches express about vdW force is play in the important role of cyclodextrin inclusion complex system. Normally the hydrophobic interactions between two non-polar molecules provide a positive enthalpy process, on the other hand, van der Waals interactions are observed as in the opposite. The negative enthalpy occurs in the van der Waals case.

According to van der Waals interaction in cyclodextrin inclusion complexes, many works consider this system in gas phase to avoid the solvent effect. While they conclude vdW interaction is the major contribution to form then inclusion complexes.

4. Hydrophobic interaction

Hydrophobic interaction in CDs complexation is a underdiscussion problem. Normally, hydrophobicity was specified to be the results of enhanced structure of the water molecules in the near vicinity of the non-polar solution, It would cause large

entropy loss during the hydration. In the experimental, non-polar molecules associate in water is normally found the positive enthalpy and positive entropy change, it seem like a signature of hydrophobic interaction. The fact that most of the experimental enthalpy and entropy alterations of CD complexation are negative seems to show that the hydrophobicity is not an important force in CD inclusion complex.

Chapter 3

Theoretical framework

In this chapter, we focus on the theoretical framework in this research. For the first step, we will start with the formulation of bindings. The method used in the calculations includes semi-empirical and *ab initio* method. Finally, the computer procedure is described, starting from the computers and softwares that are used in the simulation, as well as to preparation of the input file, monomer optimization, molecular docking simulation, binding energy analysis, Complete Basis Set (CBS), and Basis Set Superposition Error (BSSE) corrections.

3.1   Formulation of bindings

The binding energy between host-guest molecules are considered as one factor, which influence to the stability of binding of the inclusion complex molecule. In order to understanding of the binding, a lot of theoretical methods including Molecular Mechanics (MM), Molecular Dynamics (MD), and more recently, Quantum Mechanical (QM) methods such as *ab initio* and Density Functional Theory (DFT), have also been used to study the CD complexes. Sometime when the experiments are in sufficient, the computational can help us to explain the mechanism of molecular interaction. Within quantum mechanics, there are methods (semi-empirical, *ab initio*) to calculate observable energy, and to evaluate the minima point of the potential energy, which related to the stationary point or quasi-stable of relaxed geometry. The optimized geometry expresses the preferable structure or the relaxed structure of this molecule. To find the binding energy, the difference of geometry optimization energy between the inclusion complex and the monomer molecule are performed. Binding energy is one of the factor to consider whether it is preferable to form the inclusion complex. The calculation is following this equation:

$$\Delta E_{binding} = E_{complex} - (E_{host} + E_{guest}) \tag{3.1}$$

where $\Delta E_{complex}$ is the inclusion complex energy between host and guest; E_{guest} is the energy of guest molecule; and E_{host} is the energy of host or BCD and two derivatives MBCD and HPBCD. The inclusion complex with the lowest energy or negative value presents the most stable inclusion complex. On the other hand, the positive value shows that they are

unfavoable to form the inclusion complexes.

3.2   Semi-empirical methods

Generally, quantum mechanic method can be classified as *ab initio* or semi-empirical. In *ab initio*, the calculations are derived directly from theoretical principle, no experimental data included. On the other hand, semi-empirical methods are the simplified versions of Hartree-Fock theory using empirical or experiment data for the correction in order to improve the performance of the calculation. As a result, this calculation is faster than *ab initio* calculation. Semi-empirical calculations are also very successful for the organic chemistry systems, that contain a few elements in used and the very large molecule size. In semi-empirical, we use empirical parameters to evaluate SCF equation, while *ab initio* does not use such empirical calculation. There are many ways to consider the electron-electron interactions when the molecules overlaps. Normally, we can separated the interactions in three groups.

1. The extended Huckel method
   This method is the model which neglect all electron-electron interactions that can make the computation very fast but not accurate.

2. Neglect of differential overlap (NDO) model
   This method can neglect some of electron-electron interactions. The Hartree-Fock Self-Consistent Field (HF-SCF) is used to solve the Schrödinger equation with various approximations. The model includes; CNDO, INDO, MINDO/3, ZINDO/1 and ZINDO/S.

3. Neglect of Diatomic Differential Overlap (NDDO)
   This model is a modern semi-empirical model which is based on INDO and included the overlap density between two orbitals on one atom interacting with the same or another atom.

NDDO is the best level, which can maintain the higher number of multi-poles of charge and the distribution between two center atoms interaction.

Integral evaluation commonly computes from three approaches consisting of the experimental data, calculated from corresponding analytical formulas, and from suitable parametric expressions. The most realistic balance between the repulsive and attractive force in molecules is the method considering the parametric functions. MNDO (Modified Neglect of Diatomic Overlap) is the widely used method considering the valence-electron with SCF-MO uses the minimal basis set of AOs or atomic orbitals. Generally, PM3, PM6, and PM7 are also under MNDO model [49], which are usually applied in host-guest inclusion complex interactions. Consequently, this research focuses on these three methods of MNDO model:

3.2.1 Parameterized Model number 3 (PM3)

This calculation utilizes the semi-empirical method for the quantum calculation of electronic structure. This method employs modern semi-empirical model or NDDO, and it is accurate to some degree. On the other hand, previous work [50, 51] compared the accuracy for gas phase heats of formation (HOF), the results of accuracy have been shown in the increasing in the order of PM3 < PDDG < PM6. DDO is ignored in integral approximation is used for the calculation. Elements that have been parametrized in PM3 include H, C, N, O, F, Al, Si, P, S, Cl, Br, I, Ca, Ti, V, Cr, Mn, Fe, Co, Ni, Cu, Zn, Zr, Mo, Tc, Ru, Rh, Pd, Hf, Ta, W, Re, Os, Ir, Pt, and Gd. Various number metals have been parameterized in later work. The cyclodextrins inclusion complex studies get the coincide binding energy result with the experimental observations from PM3.

PM3 deals with hydrogen bond (O-H...O) and reproduces the crystalline structure relatively well [51, 52]. As a result, PM3 was selected for the calculation in several studies [50, 53] including our previous work [17]. PM6 method [54] adds some improvement of PM3 in the geometries prediction, for instance, replacing Gaussian core-core corrections to core-core correction introduced by Voityuk and Rosch [55].

3.2.2 Parameterized Model number 6 (PM6)

PM6 performs pairwise parameter and also uses different core-core repulsion potentials for N-H, O-H, C-C and Si-O which also improve some weaknesses in the parametrization. The previous studies also show good performance of this method in cyclodextrin inclusion complex system, which improves the stability of inclusion complex structure by adding damping functional [56, 57]. Some works [58] express the thermodynamic parameters results from PM6 in gas and water according to MD simulations and the experiment as results [38,59,60].

3.2.3 Parameterized Model number 7 (PM7)

PM7 method [61] improves some part of PM6 appending explicit terms to describe non-covalent interactions or non-bonding interaction, for instance, hydrophobic-hydrophobic interactions and long range bonding interaction or hydrogen bond, which is the interaction between host-guest of our system. The accuracy of this method can be compared to the higher level of theoretical methods, while requiring of low computational cost. This method also provides good results in $\Delta G°$, $\Delta H°$ and ΔS comparing to the experimental value [62]. Basically, PM7 illustrates high value of $\Delta E_{\text{HOMO–LUMO}}$ energy gap of BCD molecule with CENs-prolinate, which means that the compound is stable [63]. PM7 is also successful used to predict the parameter of geometry structure and reactive trend in complex between microcystins and nodularins with cyclodextrin [64]. On the other hand, there are some limitations of this method including large error for the non-covalent interaction energy [59].

Table 3.1: Comparison of three semi-empirical methods, PM3, PM6 and PM7.

Informations	PM3	PM6 [54]	PM7 [61]
Year	1989	2007	2012
Compounds used for parameterization Experimental data	~500	>9,000 (include *ab initio* data)	>9,000 (include *ab initio* data)
Average unsigned error (kcal/mol)*	6.23	4.42	4.01
Root Mean Square Error (kcal/mol)*	9.44	6.16	5.89
Largest error (kcal/mol)*	-135.6	-42.2	-44.4
Hamiltonians	H, C, N, O, F, Al, Si, P, S, Cl, Br, I, Ca, Ti, V, Cr, Mn, Fe, Co, Ni, Cu, Zn, Zr, Mo, Tc, Ru, Rh, Pd, Hf, Ta, W, Re, Os, Ir, Pt, and Gd+15 lanthanide sparkles (57)	H,He,Li,Be,B,C,N,O,F,Ne, Na,Mg,Al,Si,P,S,Cl,Ar,K, Ca,Sc,Ti,V,Cr,Mn,Fe,Co, Ni,Cu, Zn, Ga, Ge, As, Se, Br, Kr,Rb, Sr, Y, Zr, Nb, Mo, Tc, Ru, Rh, Pd, Ag, Cd, In, Sn, Sb, Te, I, Xe, Cs, Ba, La,Lu, Hf, Ta, W, Re, Os, Ir, Pt, Au, Hg, Tl, Pb, Bi +15 lanthanide sparkles (83)	H,He,Li,Be,B,C,N,O,F, Ne,Na,Mg,Al,Si,P,S,Cl, Ar,K,Ca,Sc,Ti,V,Cr,Mn, Fe,Co,Ni,Cu, Zn, Ga, Ge, As, Se, Br, Kr,Rb, Sr, Y, Zr, Nb, Mo,Tc, Ru, Rh, Pd,n Ag, Cd, In, Sn, Sb,Te, I, Xe, Cs, Ba, La, Lu, Hf,Ta, W, Re, Os, Ir, Pt, Au, Hg, Tl, Pb, Bi +15 lanthanide sparkles (83)
Hydrogen bond	H atom is in correct displaced indicate a single bond to one O.	PM6 method fails for the description of non-covalent interactions, dispersion energy and H-bond	H-bond more accurate, consistent with experiment observation and DFT geometries
Basis set for valence	s, p	s, p, d	s, p, d
Dispersion force prediction	None	Poor (core-core replusion term revised)	Quit good (with GD2 correlation similar to GD3)

Comparison of errors in heats of formation for a set of 1,366 compounds containing only C, H , F, O, N, Br, S, P and Cl.

Table 3.1 illustrates the comparison between three semi-empirical methods (PM3, PM6 and PM7). The information is from MOPAC, the semi-empirical program website developed by Stewart [54, 61]. We can see the development of the PM version from the starting, which including the number of compound used for parameterization. PM6 and PM7 included the immense number of data which are from the experimental and *ab initio* method. The errors were reduced that we can notice by the decrease number of Average unsigned error, Root Mean Square Error and Largest error. Finally, the dispersion energy were include in to PM7 method, which is the newest version of PM series.

3.3 *Ab initio* method

Ab initio quantum chemistry is an important tool to study atoms and molecules, where the number of studies have been increasing every year in the material and biology area. The main idea of this tool is the computational solution derived directly from theoretical principles or electronic Schrödinger equation, and the calculations exclude experimental data. To find "good-enough" solutions of electronic Schrödinger equation to explain some systems, many of theoretical chemistry have been performed. It is an approximations, that are usually mathematical approximations using a simple functional form to find approximate solution from differential equation.

Many types of *ab initio* methods have been used nowadays. Popular *ab initio* methods comprise Molecular orbital (MO), Density Functional Theory (DFT) and Quantum Monte

Carlo (QMC). Normally, *ab initio* provides a good qualitative results and also increasingly the accuracy in qauntitative results. It is very useful for providing the initial, the first level of prediction. The structures and vibrational frequencies of stable molecules and transition states are performed reasonably. However, this method neglects of electron correlation makes it unsuitable for some purposes. For example, it is insufficient for accurate modeling of the energetic of reactions and bond dissociation.

There is some senses that one would not expect any empirical data to be included within an *ab initio* framework. In reality, *ab initio* methods regularly utilize insights gained from empirical observation. This can be seen, for example, in the B3LYP exchange-correlation functional and others (Minnesota Functionals, DFT-GD3), which include empirical parameters and fitting. Approximations are also featured regularly in *ab initio* methods. Here it is evident that *ab initio* does not necessarily mandate a rigorous derivation from purely theoretical grounds. Having mentioned this, *ab initio* methods are most rigorous with respect to the theoretical principles, much more so than semi-empirical and empirical methods. The approximations utilized within *ab initio* are generally numerical in nature, approximating numerical equations instead of the physical picture. These approximations are geared more toward reducing computational costs instead of modelling a physical reality. As a result, it can be said that *ab initio* methods do not aggressively use approximations. This tendency is the distinct characteristic of *ab initio* methods.

3.3.1 Basis set

To describe the shape of atomic orbital of our target system, the basis set of wave function is required. The level of approximation is related directly to our selected basis set. Therefore, we have to balance between the CPU time and accuracy of our results. In this thesis, we consider Gaussian basis set. Figure 3.1 represents two types of orbital, the first one is Slater Type Orbitals (STOs), which can explain shape of AOs closely than the Gaussian Type Orbitals (GTOs). However, GTOs is easier and faster to compute and combine numerous orbital than STOs. Hence, GTOs are commonly used to describe AOs than STOs [65].

Slater function
$$s_\nu(\mathbf{r}) = e^{-\zeta_\nu |\mathbf{r}|} = e^{-\zeta_\nu \sqrt{(x^2+y^2+z^2)}}$$

Gaussian function
$$g_\nu(\mathbf{r}) = e^{-\zeta_\nu \mathbf{r}^2} = e^{-\zeta_\nu (x^2+y^2+z^2)}$$
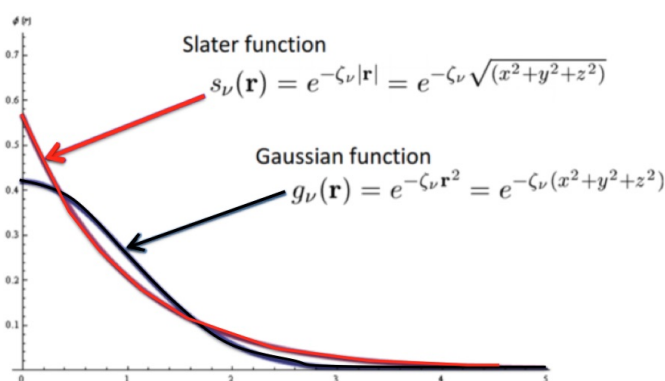
Figure 3.1: Schematic of Slater and Gaussian function, figure is taken from literature [8].

Minimal

To explain the atomic orbital, this kind of basis set uses only one functional or STO to describe it. STO-nG, where n = 2,...,6. (usually n < 3 provide too poor results) n GTO are used to describe by STO. Therefore, STO-3G is the minimal basis set. The minimal basis set is used when our target system is very small, or we want to find the qualitative result of the huge target system.

Split Valence

The most popular one normally used for organic molecules is called Pople basis sets. For this basis set, we can select number of GTO used for core and valence electron. The notation is K-LMG, where K presents the number of sp-type (inner shell GTOs). The notation of L means the number of $s-$ and $p-$type of inner valence. M indicates $s-$ and $p-$type of outer valence. Finally, G means that GTOs type is used. For instance, 6-31G : 6 GTOs are set for core, while 3 GTOs are used for inner valence and 1 GTOs explains the outer valence electron. Gaussian program consist many types of split valence, such as 3-21G, 4-31G, 4-22G, 6-31G, 6-311G, 7-41G etc.

To make the setting better describing the target system, we can set the electron movement, far or near the nucleus by setting diffuse orbitals. This setting is used to excite the state and our molecules consisting of lone pair and anion case. We can set it by adding plus (+) and double plus sign (++) in front of G. ++ means diffuse functions adding to all atom while + means diffuse functions adding to all except hydrogen atom.

The polarization also can be set to our target system, which can be set by adding *, ** or (d) and (d, p). This setting is set when our target system get polarized from surrounding case. * or (d) means d-type functional adding on atom except hydrogen atom and f-type function is added to transition metals. ** or (d, p) indicates p-type functionals are added to hydrogen and d-type functionals are added to other atoms. Finally f-type functionas are added to transition metal.

3.3.2 Time-independent many-particle Schrödinger equation

For time-independent many-particle Schrödinger equation can be presented as:

$$\hat{H}\Psi = E\Psi \tag{3.2}$$

where, $\hat{H}$ is Hamiltonian operator and Ψ is a set of solutions, which is $\Psi(\vec{r_1},...,\vec{r_N})$, or eigenstates of the Hamiltonian. The solutions related to eigenvalue, E_n is a real number that satisfies the eigenvalue equation. If we consider further like particle in a box or harmonic

oscillator, the complete description of the Schrödinger equation is

$$\left[-\frac{\hbar^2}{2m} \sum_{i=1}^{N} \nabla_i^2 + \sum_{i=1}^{N} V(\vec{r}_i) + \sum_{i=1}^{N} \sum_{i<j} U(\vec{r}_i, \vec{r}_j) \right] \Psi = E\Psi \tag{3.3}$$

Three terms are defined as follows:

- $-\dfrac{\hbar^2}{2m} \Sigma_{i=1}^{N} \nabla_i^2$ is the kinetic energy operator of each electron.

- $V(\vec{r}_i)$ is the interaction energy between each electron and the collection of atomic nuclei.

- $U(\vec{r}_i, \vec{r}_j)$ is the interaction between different electrons.

Ψ is the electronic wave function of each spatial coordinates of each of the N electrons, $\Psi = \Psi(\vec{r}_1, ..., \vec{r}_N)$ and E is the ground state energy of the electrons. The electron wave function is a function of each of the coordinates, of all N electrons, it is possible to map this many-body, interacting problem to a set of one-body noninteracting problem (Kohn-Sham equations) as described below.

3.3.3 Kohn-Sham Equations

In principle, the ground-state energy is also solved by minimizing the total energy with all state $|\Psi\rangle$, with density $n(\vec{r})$.

$$\begin{aligned} E[n] &= \min_{\Psi \to n(\vec{r})} [\langle \Psi | \hat{T} | \Psi \rangle + \langle \Psi | \hat{V}_{int} | \Psi \rangle] + \int d\vec{r} V_{ext}(\vec{r}) n(\vec{r}) \\ &\equiv F[n] + \int d\vec{r} V_{ext}(\vec{r}) n(\vec{r}) \end{aligned} \tag{3.4}$$

V_{ext} is the external potential while $F[n]$ is universal functional and it is difficult to find this part. Therefore, it is corresponding for solving many-particle following the Kohn-Sham equation. This equation considers complications of many-body effects in interacting system as in $F[n]$, which contains a few correction to total energy of auxiliary system with the many-body effects. DFT can be rewritten for ground-state energy as functional of density the following equation:

$$E_{aux}[n] = T_s[n] + E_H[n] + \int d\vec{r} V_{ext}(\vec{r}) n(\vec{r}) \tag{3.5}$$

$$T_s = -\frac{1}{2} \sum_{i=1}^{N} \langle \phi_i | \nabla^2 | \phi_i \rangle$$

$$E_H = \frac{1}{2} \int d\vec{r} d\vec{r'} \frac{n(\vec{r}) n'(\vec{r})}{|\vec{r} - \vec{r'}|} \qquad (3.6)$$

$$n(\vec{r}) = \sum_{i=1}^{N} |\phi_i(\vec{r})|^2$$

where, the one-electron wave function ϕ_i is considered in the auxiliary system. It is similar to ground state density to original system. The auxiliary system should be changed into the manners that present many-body effects. It will also be available in the real physical system. As a result, Kohn and Sham have also given a name as the exchange-correlation functional $E_{XC}[n]$ which can be expressed in terms of F as

$$F[n] = T_s[n] + E_H[n] + E_{XC}[n] \qquad (3.7)$$

where T_s is the kinetic energy of independent particles. E_H is the self-interacting energy of electron density and E_{XC} is the exchange correlation energy. Non-zero exchange-correlations, and Hamiltonian of original auxiliary are not practicable for this case. However, before the single-particle wave functions can be obtained, $\hat{H}$ can be changed according to the effect of exchange-correlation term.

3.3.4 Exchange and Correction Functionals

DFT concept is principle exact, although in practical is approximation. The approximation is from the electron interaction between each other. The interactions are approximated, what we called exchange-correlation (XC) functionals. There are many functionals try to approximate this interaction as accurate as possible as follows:

1. Local Density Approximation (LDA)

   The oldest and simplest functional of DFT, LDA is based on the uniform or homogeneous electron gas. The exchange-correlation energy density is assumed as every position in molecule space as same as uniform electron gas (UEG) containing the same energy in every position.

$$E_{XC}^{LDA}[n] = E_X^{LDA}[n] + E_C^{LDA}[n] \qquad (3.8)$$

   The exchange energy is as the following equation:

$$E_X^{LDA}[n] = C \int n^{\frac{4}{3}}(\vec{r}) d\vec{r} \qquad (3.9)$$

   The exchange energy depends only on its electron density at the given position, which

make the calculation were simple. As a result, the LDA calculation is very fast and often provides a good geometries. However, sometimes the results provide systematic errors in energy from the stronger bonds or overbinds.

2. Generalized Gradient Approximation (GGA)

Commonly, GGA provides the improved results from LDA. This functional is divided into two parts, exchange and correlation functionals, and also derived separately. The exchange energy does not depends on the value of density at a point as in LDA, but depends on its gradient as follows:

$$E_{XC}^{GGA}[n] = \int n(\vec{r})\varepsilon_{XC}(n(\vec{r}),|\nabla n(\vec{r})|)d\vec{r} \tag{3.10}$$

Most of GGA functionals are constructed from LDA functional and added the correction term as the follows:

$$\varepsilon_{XC}^{GGA}[n] = \varepsilon_{XC}^{LDA}[n] + \Delta\varepsilon_{X/C}\left[\frac{\left|\nabla n(\vec{r})\right|}{n^{\frac{4}{3}}(\vec{r})}\right] \tag{3.11}$$

If the functionals contain empirical parameters, the values are fitted to reproduce the experimental result, such as exchange B(Becke), CAM, FT97, O, PW, mPW, X. Correlation B88, P86, LYP. On the other hand, the functionals exclude the empirically determined parameter as the the following: exchange B86, LG, P, PBE, mPBE. Correlation is PW91.

3. Hybrid Exchange Functionals

These functionals include fractions of exact Hartree-Fock exchange energy, which calculated as a functional of the Kohn-Sham molecular orbitals. The general form is from the following equation:

$$E_{XC} = (1-a)E_{XC}^{DFT} + aE_X^{HF} \tag{3.12}$$

The most successful functional is B3LYP 3-parameter functional or Backe3LYP. In 1993, Becke introduced the first hybrid functional between some exact HF exchange with GGA exchange. This functional is the most widely used for molecular calculations, especially for many organic molecule calculations.

$$E_{XC}^{B3LYP} = (1-a)E_{XC}^{LDA} + aE_X^{HF} + b\Delta E_X^{B} + (1-c)E_c^{LDA} + cE_c^{LYP} \tag{3.13}$$

where $a = 0.1161$, $b = 0.9262$ and $c = 0.8133$. Basically, there are many hybrid functionals, for instance B1PW91, B1LYP, B1B95, mPW1PW91 and PBE1PBE

3.3.5 Dispersion Functional

To consider the interaction between two molecule in organic system, non-covalent interaction such as dispersion or van der Waals and hydrogen bond play an important role. However the conventional DFT cannot estimate the long-range dispersion interaction. Dispersion energy arises when electrons move and induce dipole, which can affect to the instantaneous charge fluctuations. To correct asymptotic behavior ($-C_6 R^{-6}$) of long-range interaction, that cannot describe by local and semi-local approximation of conventional DFT, thus some functionals were developed their approximation to describe these interactions.
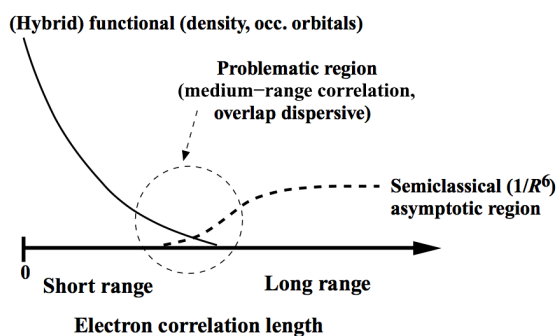
Figure 3.2: Schematic classification of the correlation and dispersion problems on different electron correlation length, figure is taken from literature [9].

There are various approaches, which we can group into 4 classes:
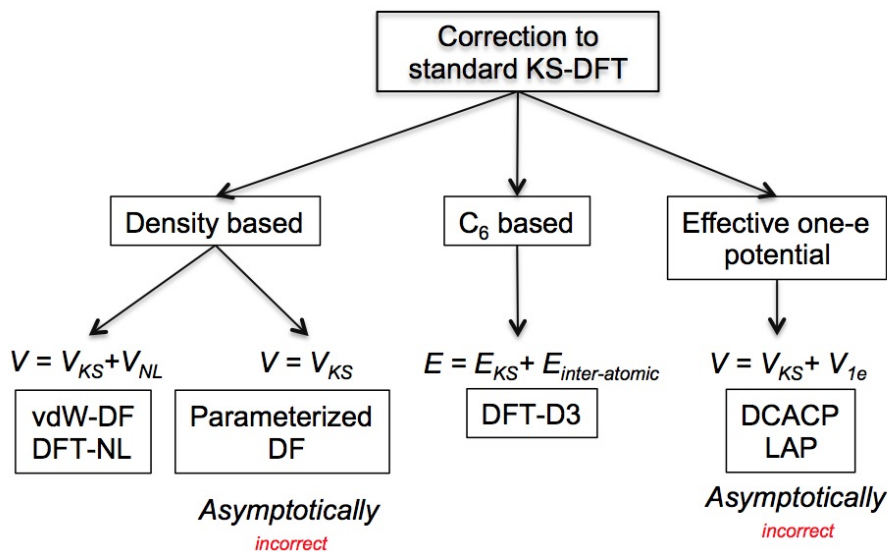
Figure 3.3: DFT dispersion correction which currently used, adapted from [9]. All four methods are used and compared in this study.

1. The vdW-DF and related methods

    Nowadays, this group is widely used, in which the method is nonempirical to solve the dispersion energy for inconsistency systems. In order to get the interaction energy, a

supermolecular calculation of the total energy of monomers molecule and complex are executed. For all vdW-DF schemes, E_{XC}, a related total exchange-correlation energy can be derived from following equation [9].

$$E_{XC} = E_X^{LDA/GGA} + E_C^{LDA/GGA} + E_C^{NL} \qquad (3.14)$$

The calculation of short-ranged parts utilize the semi-local (GGA) and local density approximation (LDA) type are correlation components and the standard exchange. A nonlocal term describing the dispersion energy is shown by E_C^{NL}, which is the modern versions of undamped. In addition, it can be a factor in correlation energy form electron-electron distances. Therefore, a normal (covalent) thermochemistry can be influenced by this type correction.

2. Conventional and parameterized Functionals (DFs)

In order to describe dispersion effects in further detail, these functionals are modified versions of regular metahybrid approximations. The modifications include an accounting of estimated kinetic energy density. For instance, Zhao and Truhlar [66] examined 18 dispersion functionals, for calculation bond length and binding energy for rare-gas dimer, alkaline earth metal dimers, zinc dimer, and zinc-rare gas dimers. In addition, M05-2X57 [67] and MPWB1K58 [68] are the methods for to predict the vdW interactions of rare-gas and 17 metals. A study of novel DFT methods has determined a set of 13 biological relevance complexes. As a result, the sensible outcomes are obtained for the stacked arrangements in the amino acid pairs and DNA base pairs, on the contrary of prior DFT methods that suffer to represent the interactions in stacked complexes. Currently, the highest accuracy of dispersion-uncorrected functional is the M06-2X functional which can provide better results for the S22 set along with the structures of stacked aromatic [69].

3. Semiclassical Correction (DFT-D)

This method utilizes the quantum chemical approach to combine the result of potential while treating the dispersion interactions semiclassically. Recently, several literatures have presented many enhanced version of DFT-D, based on an atom pairwise additive treatment with dispersion energy [9]. The following equation shows the general form of dispersion energy:

$$E_{disp}^{DFT-D} = -\sum_{AB} \sum_{n=6,8,10,...} s_n \frac{C_n^{AB}}{R_{AB}^n} f_{damp}(R_{AB}) \qquad (3.15)$$

where, R_{AB} is the distance of internuclear. While, C_n^{AB} presents the averaged dispersion coefficient (isotropic n^{th}-order n of 6, 8, 10, ...) for atom A and B. s_n is global scaling factors (DF-dependent), which is used to adjust the repulsive behavior. f_{damp}

or damping functions, which used to determine range of dispersion correction. Finally, the summation is total atom pairs in the system.
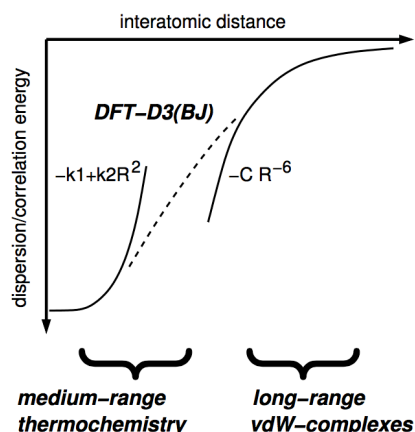
Figure 3.4: Schematic of short- and long-range behavior of dispersion interaction, figure is taken from literature [9].

The most popular method is DFT-D, first represented with the version DFT-GD1 in 2004. Subsequently in 2006, the DFT-GD1 has been updated to DFT-GD2. Futhermore, DFT-GD3 method, the next verion, is a modification with less empiricism, broader range of applicability and higher accuracy. Computed from first principles, a new set of cutoff radii and coefficients of atom pairwise-specific dispersion are the modern components. The enhanced method of DFT-GD3 have been used in the computation of molecular dispersion energy, electronic structure and solids with DFT. In arbitrary systems at present, the DFT-GD3 is simplest method for such data computation.

4. One-Electron Corrections (1ePOT)

The concept is from von Lilienfeld [70], by utilizing the optimized, atom-centered nonlocal potentials (DCACP) deployed in the pseudopotentials for core electrons context. This method is used to model the long-range vdW forces presented for benzenebenzene, argonargon, argonbenzene, graphitegraphite complexes. Nevertheless, this method rapidly decays and presents incorrect asymptotic R^{-6} behavior. Additionaly, it is a defective approach becuase of fixed atomic parameters in each element. As a result, it is unable to return the dispersion coefficients changes with the hybridization of an atom in a solid molecule.

3.4   Justifications for the methods

To select the suitable calculation basis sets and method for our system is very important before the calculations are performed. Many factors need to be considered and literatures

Table 3.2: Mean Absolute Deviations (MADs, in kcal/mol) for common dispersion-corrected DFT methods.

Method	Type of DF	Class	MAD	Ref
ω B97X-D	Hybrid GGA	III	0.22	[71]
BLYP-GD3	GGA	III	0.23	[72]
vdW-DF (optB88)	GGA + nonlocal	I	0.23	[41]
LC-BOP + LRD	Hybrid GGA	III	0.27	[6]
B2PLYP-GD3	Double hybrid	III	0.29	[72]
B3LYP-GD3	Hybrid GGA	III	0.46	[72]
M06-2X	Meta-hybrid GGA	II	0.41	[69]
vdW-DF (PBE)	GGA +nonlocal	I	1.19	[73]

also need to be reviewed to make the reasonable system for the calculation. As the result, before performed the large calculations, semi-empirical calculation was used to performing the first step to find the possibility to form the inclusion complex of this system. This step is good for large systems such as cyclodextrin inclusion complex. According to Table 3.3 and 3.4, many previous works were performed with PM3, because of better performance to perform hydrogen bond comparing to other semi-empirical method such as AM1. PM6 and PM7 are also the improved version of PM3. Hence, this research is focused on three types of semi-empirical methods for the first phase of the calculation.

3.4.1 DFT functionals

The next step, *ab initio* calculation was performed. DFT calculation with hybrid functional or B3LYP was selected. B3LYP functional is widely used for molecular calculations for many organic molecule calculations. This functional also provides better geometry optimization structure. As a result, the final structure after performed geometry optimization is uniform. Nevertheless, this functional cannot express long-range or the interaction between the molecule well. Then, five functionals were considered further, including; CAM-B3LYP, B3LYP-GD3, CAM-B3LYP-GD3, M06-2X, and M06-2X-GD3. Each functionals included the long-range or dispersion part in the calculation, except B3LYP. The further information is as follows:

- CAM-B3LYP

  Generally, CAM exchange correlation functional uses long-range correlation concept. The key of long-range correction for DFT is the DFT exchange included two terms: short-range and long- range (orbital-orbital). The long-range term is from Hartree-Fock (HF) exchange integral. Yanai et al. believe the functional can predict energetic quantities more accuracy than B3LYP Yanai *et al.* [74]. In our work, CAM correction also provides better result of binding energy than B3LYP. The slight improvement

is found in our target system. Nevertheless, Okuno *et al.* stated that this functional is powerful and providing a reliable excited state calculation with molecule structure optimized by B3LYP method [75]. Additionally, for the dynamic hyperpolarizabilities, CAM correction also provides the accurate results while Limacher *et al.* also mentioned that this functional provides a good molecular geometry comparing with experimental structures (for longer chain lengths) [77]

- B3LYP-GD3, CAM-B3LYP-GD3 and M06-2X-GD3
  For B3LYP-GD3, we can label this method as DFT-GD3 [72]. Commonly, the overall of DFT-GD3 energy can be derived from the following equation:

$$E_{DFT-GD3} = E_{KS-DFT} - E_{disp}, \tag{3.16}$$

where E_{KS-DFT} commonly represents a self-consistent KS energy obtained from selected DF, while E_{disp} is a dispersion correction. The dispersion term is illustrated as in Equation 3.15. The previous research from Chen *et al.* [78] and Witte *et al.* [79] also illustrated the functional with GD3 correction with better performance than BLYP and the previous functional. The improvement from damping functions are significantly reducing the errors associated with non-covalent interaction energies and geometries.

The DFT-GD3, the exchange correlation functional, is the improved version from DFT-GD2. The key improvement is the larger of cutoff atomic radii. This factor affects the distance range of dispersion correction using damping function. DFT-GD3 can fix the over binding of DFT-GD2 result and the result will become almost identical, and significantly improves nearly to CCSD(T) reference data results [72]. This method can handle van der Waals complexes and the intermolecular non-covalent interaction, while the calculation is extremely robust, fast and numerical stable. However, this method unable to cover the thick metal slabs or anisotropic structures with zero electronic energy gap, because it cannot cover in enough component of the fluctuations on the extensive space dimension [80].

- M06-2X
  This functional, based on the meta-GGA approximation, was developed from Minnesota Functionals group at the University of Minnesota leading by Prof. Donald Truhlar [66]. The terms in the functional, based on the complex functional forms parametrized to the databases with high-quality benchmark, depending on the density of kinetic energy. M06-2X, a high non-locality functional with double the amount of nonlocal exchange, is in Minnesota 06 family with a general improvement over the 05 family parametrized only for nonmetals. It is 54% HF exchange global hybrid functional efficiently under the 06 functionals for non-covalent interactions, kinetic, and thermochemistry. However, this functional is unable to employ with transition

metal thermochemistry and organometallic. M06-2X is recommended functional to study the non-covalent interactions, since it can provide the smallest BMUEs for the NCIE53 database [69].

3.4.2 Basis sets

A basis set is a set of mathematical functions that a wave function can be constructed. For higher efficiency, three considerations have to be concerned:

1. The number of two electron integrals increase as N^4 where N is the number of basis functions. As a result, the total number of basis functions need to be consider as a minimum of computational attractive;

2. A larger basis set presents a computer improvement which is better than a small basis set. We have to evaluate between the the computational improvement or the speed;

3. In the end, the basis set functions need to be be selected to benefit as in a chemical sense. The function should be large amplitude in region and space sufficiently.

Most semi-empirical methods use a predefined basis set. On the other hand, the *ab initio* (DFT) requires specified basis set. Normally, the existing basis sets are used for the calculation. Commonly, STO-3G set is the famous smallest basis set (minimal basis set). Therefore it seems not sufficient for our target system.

Another type of basis sets, indicated by the notation 6-31G, are the Pople basis sets which we mention in Section 3.3.1. These famous basis sets are particularly used with organic molecules. For polarization functions, the notation of Pople basis set can be altered by appending asterisks, for example, 6-31G** or 6-31G*, in order to provide adaptibility to change shape for the wave function. The variational total energy normally reduces when appending polarization functions in the similar amount of another contraction attachment. The higher geometries computation accuracy and vibrational frequencies can be obtained as the results of polarization functions. Our target system is suit to consider diffuse functions,

which are utilized for anions with larger distributions of electron density and for describing long distances interactions (van der Waals interactions). Appending the diffuse functions can impact the alteration of relative energies for variety of geometries related to the systems [52, 81]. The small 6-31++G** basis set was selected as it provides the better dissociation energies for covalent bonds. The utilization of a relatively small 6-31++G** basis set leads to significant over binding for all the tested functionals. This effect can be partially compensated by including the BSSE corrections [65].

Table 3.3: Literature review of the basis sets which are used in the cyclodextrins case studies.

Topic	Host/Guest	Calculation program	Basis set	Reference
Theoretical and experimental study of the tetracain/BCD inclusion complex	BCD/tetracain	Gaussian03	PM3 HF/6-31G(d)	[82]
Twisted intramolecular charge transfer effects on fast violet B and fast blue RR: Effect of HPACD and HPBCD	HPBCD/violet B	Gaussian03	PM3	[83]
Modeling of the inclusive complexation of natural drug trans 3,5,30,40-tetrahydroxystilbene with BCD	BCD/3,5,30,40-tetrahydroxystilbene	Gaussian 09	PM3 B3LYP/6-31G*	[48]
Studies on inclusion complexation between 4,40-dihydroxybiphenyl and BCD by experimental and theoretical approach	BCD/4,40-dihydroxybiphenyl	Gaussian03	PM3	[84]
Host-guest inclusion complex between BCD and paeonol: A theoretical approach	BCD/paeonol	Chem3D Ultra	PM3 ONIOM2 (B3LYP/6-31G*), (HF/6-31G*:PM3)	[85]
Inclusion complexes of cefuroxime axetil with BCD: Physicochemical characterization, molecular modeling and effect of l-arginine on complexation	BCD/cefuroxime axeti	VLifeMDS4.3 software Suit	Merck Molecular Force Field	[86]
Biomimetic asymmetric Michael addition reactions in water catalyzed by amino-containing BCD derivatives	BCD/Biomimetic asymmetric Michael	ChemBioOffice 3D	PM3 B3LYP/6-31G(d)	[87]
A combined DFT and experimental study of proline/BCD inclusion complex	BCD	Chem-Office 3D ultra	DFT (B3LYP/3,21G+ level)	[88]
Computational Molecular Perspectives on the Interaction of Propranolol with BCD in Solution: Towards the Drug-Receptor Mechanism of Interaction	BCD/solution	Gaussian09	SQM(PM3 and PM7) DFT(631G) B3LYP hybrid exchange3-21G and 6-31G ONIOM (DFT,SQM(PM3))	[62]
A hybrid MP2/DFT scheme for N-Nitroso-N-(2-chloroethyl)-N'-sulfamoylprolinate/BCD supramolecular structure: AIM, NBO analysis	BCD/N-Nitroso-N-(2-chloroethyl)-N'-sulfamoylprolinate	Gaussian09	PM7 hybrid calculation (DFT/DFT) and (MP2/DFT) combinations B3LYP/6-31G*	[63]
BCD as an additive to improve the thermostability of Yarrowia lipolytica Lipase 2: Experimental and simulation insights	BCD/Yarrowia lipolytica Lipase 2	Gaussian03	HF/6-31G(d) After than run MD calculation	[89]
Thermal analysis and theoretical study of Alpha-cyclodextrin azomethine [2]-rotaxane formation by semi-empirical method PM3	ACD/rotaxane	HyperChem	PM3	[90]
Molecular modeling investigation of para-nitrobenzoic acid interaction in beta-cyclodextrin	BCD/para-nitrobenzoic	Gaussian03	MM+ PM3 DFT/B3LYP/6-31G(d)	[37]

Table 3.4: Literature review of the basis sets which are used in the cyclodextrins case studies.

Topic	Host/Guest	Calculation program	Basis set	Reference
Structural and theoretical-experimental physicochemical study of trimethoprim/randomly methylated-beta-cyclodextrin binary system	MBCD/trimethoprim	CaChe Worksystem 6.1 MOPAC2009	MM3 AM1, PM3, RM1 PM6 and PM3-D Calculation	[91]
Inclusion complexes of HPBCD with agomelatine: Preparation, characterization, mechanism study and in vivo evaluation	HPBCD/agomelatine	Autodock 4.2 Gaussian09 ChemBioDraw Ultral 14.0 molecular	MMFF94 force field (normally use in Protein field)	[92]
Computational study of inclusion complex formation between carvacrol and BCD in vacuumand in water: Charge transfer, electronic transitions and NBO analysis Lahcene	BCD/carvarol	Chem-Office 3Dultra (version 10, Cambridge Software)	PM3	[39]
Fluorometric and theoretical studies on inclusion complexes of BCD and d-,1-phenylalanine	BCD/L-phenylalanine	Gaussian03	PM3	[50]
Inclusion complex of N-nitroso, N-(2-chloroethyl), N, N-dibenzylsulfamid with beta-Cyclodextrin: Fluorescence and molecular modeling	BCD/N-nitroso	Hyperchem 7.51 Gaussian03W version 6.0	MM+ + PM3	[93]
Encapsulation of serotonin in b-cyclodextrin nano-cavities: Fluorescence spectroscopic and molecular modeling studies	BCD/Fluorescense	HYPERCHEM 7.5	AM1	[94]
Excimer formation in inclusion complexes of BCD with salbutamol, sotalol and atenolol: Spectral and molecular modeling studies	BCD/salbutamol, sotalol and atenolol	Gaussian03W Spartan 08	PM3 + Single point HartreeFock	[53]
Thermodynamic study of -cyclodextrin-dye inclusion complexes using gradient flow injection technique and molecular modeling	BCD/	MOE, DS2.5	CHARMM force field	[95]
Inclusion Complexation of Acetanilide into the BCD Nanocavity: A Computational Approach	BCD/Acetanilide	Gaussian03	PM3	[96]
Molecular modeling study of Lamotrigine/Beta-cyclodextrin inclusion complex	BCD/Lamotrigine	Hyperchem 7.51 Gaussian03 W version 6.0	MM+ AM1, PM3 B3LYP/3-21G and 6-31G	[97]
Multimodal molecular encapsulation of nicardipine hydrochloride by BCD, HPBCD and triacetyl-BCD in solution. Structural studies by 1H NMR and ROESY experiments	BCD, HPBCD/nicardipine hydrochloride	ChemOffice Ultra 6.0	MM2 force field method	[98]

3.5 Molecular Docking Simulation

There are many possibles conformations, that host and guest can be formed. The different initial geometry will provide the difference results. If there are some tools, that can predict the possible conformation must be easier to select the complex to run further calculations. Autodock is one tool, which predict how match between ligand and the host which is the biomacromolecular molecule from the interaction between them. Normally this program is used in computer-aided drug design to find the candidate molecule with their targets. Search and score method are used for finding the configuration space available for interaction between ligand and host. Evaluation the occurrence, the scoring system is used to find the binding energy.

Autodock4.2.6 use the Lamarckian Genetic Algorithm and empirical free energy to scoring the result. Scoring function makes the calculation faster, that can be used for the larger systems. A semi-empirical free energy force field is used for evaluating the conformation during the docking simulation. The force fields were parameterized by the large number of protein and inhibitor complexes in to inhibition constants or K_i.
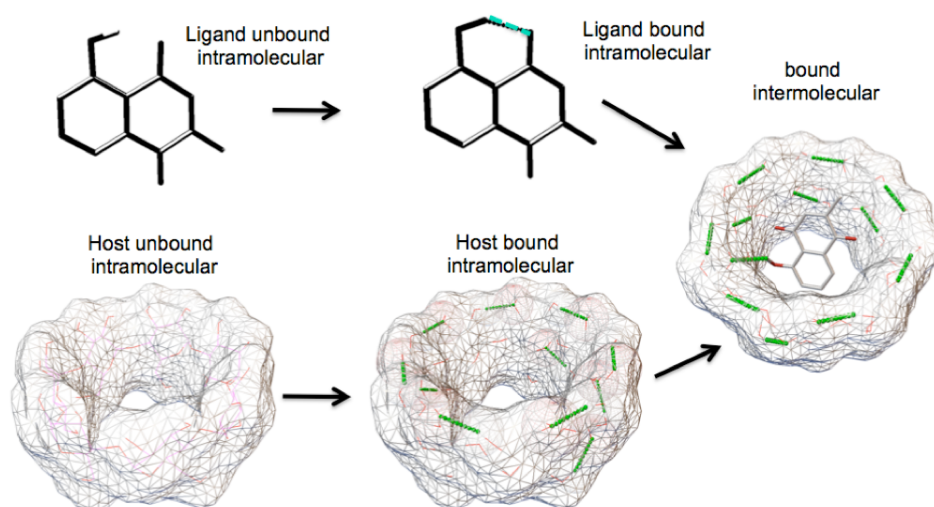
Figure 3.5: Force field evaluated binding of the molecules in two steps, the first is intramolecular force in monomer molecule and then the intermolecular force between ligand and host are evaluated.

The force field includes six pair-wise evaluations (V) and the conformational entropy lost during the formation (ΔS_{conf}) , where L means ligand, P mean Protein and P-L is the conformation between ligand and protein.

$$\Delta G = (V_{bound}^{\text{L-L}} - V_{unbound}^{\text{L-L}}) + (V_{bound}^{\text{P-P}} - V_{unbound}^{\text{P-P}}) + (V_{bound}^{\text{P-L}} - V_{unbound}^{\text{P-L}} + \Delta S_{conf}) \qquad (3.17)$$

For each of pair-wise energetic terms evaluate all of the energy from dispersion-repulsion,

hydrogen bonding, desolvation and electrostatics as the following equation. W is the weight constant, which is evaluated from the optimization of semi-empirical free energy based on the binding constant from the experimental data.

$$V = W_{vdW} \sum_{i,j} \left(\frac{A_{ij}}{r_{ij}^{12}} - \frac{B_{ij}}{r_{ij}^6} \right) + W_{h-bond} \sum_{i,j} E(t) \left(\frac{C_{ij}}{r_{ij}^{12}} - \frac{D_{ij}}{r_{ij}^{10}} \right) + W_{elect} \sum_{i,j} \frac{q_i q_j}{e(r_{ij}) r_{ij}} + W_{sol} \sum_{i,j} (S_i V_j + S_j V_i) e^{(-r_{ij}^2/2\sigma^2)} \tag{3.18}$$

The first term is dispersion and repulsion interactions (6/12 potential for dispersion/repulsion interaction), which the parameter based on Amber force field. The second term is hydrogen bond term; C and D are the maximal of bonding, hydrogen bond with oxygen and nitrogen is 5 kcal/mol (1.9Å) for hydrogen bond with sulfur is 1 kcal/mol (2.5Å). The function $E(t)$ base on the angle t, which in the ideal position of hydrogen. The third term is the screen Coulomb potential for electrostatics. For the forth term, the desolvation potential, which base on volume (V) and solvation parameter (S) and exponential term is distance weighing factor σ =3.5Å.

The genetic algorithm (GA) is used to describe in orientation, translation and conformation of ligand and protein arrangement [99]. The algorithm begins after created the random population of individuals, which are set by the user. The orientations are given a random in unit vector and rotation angle between -180 and +180 degree. In addition, there is a number generator, which is the independent hardware. It produces the random initial population follow by loop over generations and repeat until reach the maximum number of evaluation. The most recent generator, which AutoDock4.2.6 used, is LGA or Lamarckian Genetic Algorithm. This algorithm use Darwinian evolution as the major characteristics and apply the Mendelian genetics.

3.6   Computational Procedure

The methodology of the research is start from the input preparation, after that optimize the monomer molecules. AutoDock program is used to find the possible conformation of the inclusion complex by setting the fixed host and movable guest. After we know the possible conformations, the optimization of the possible inclusion complex begins. Next, we calculated the binding energy and consider the thermodynamic parameters to analyst the results. Computer-aided molecular modeling is used to find out binding interaction and thermodynamics properties of interested complex system. The procedure start from when the

X-ray structures of the hosts are downloaded, and guest molecule was constructed. All of the monomers molecules were optimized their geometry by using six functionals; CAM-B3LYP, B3LYP-GD3, M06-2X, M06-2X-GD3, CAM-B3LYP-GD3 and B3LYP with 6-31++G(d, p)

basis set. Then, two types of conformations (up and down) of each inclusion complex were optimized the geometry by using the same functionals and basis sets. Finally, BSSE calculation were performed by using the last conformation of the inclusion complexes.

3.6.1 Computers and softwares

Computers for Calculation

- Two computers with Intel Core i7-3770 CPU @ 3.40GHz (4 cores), 8 GB RAM, Windows 8, Intel display graphics 4000.

- Two computers with Intel Core i7-4790 CPU @ 3.60GHz (8 cores), 8 GB RAM, Ubuntu 14.04 LTS, NVIDIA GeForce GT 720/PCIe/SSE2.

- JAIST's HPC Fujistu CX250 cluster Intel Xeon E5-2680v2 2.80GHz (10 cores)x2, 64 GB(4GB DDR3-1866 ECCx16), overall systems 108 nodes (216 CPU/2160 cores).

- JAIST's HPC Fujistu SGI UV3000 cluster Intel Xeon E5-4655v3 2.90GHz (6 cores, 30M), 256 GB (256 CPU/1536 cores).

Software

- GaussView5.0 [16] and Gaussian09 [15] program package for structural construction and optimization of small molecules.

- Discovery Studio Visualizer 4.0 [100] to perform structural superimposition and visualize the protein-ligand interactions.

- AutoDock4.2.6 [101] to calculate the probably conformations between ligands and hosts.

3.6.2 Structure preparation and optimization

Guests compound molecule structures were constructed by GaussView5.0. All of Cyclodextrin molecules structure obtained from Cambridge Crystallographic data file (CCDF) [102]. The structure including BCD, MBCD and HPBCD were downloaded as follows:

- BCD, using BCDEXD03 or β-Cyclodextrin hydrate clathrate [103];

- MBCD, BOYFOK04 or heptakis(2,6-Di-O-methyl)-β-cyclodextrin pentadecahydrate [12];

- HPBCD, KOYYUS or 2-O-((S)-2-Hydroxypropyl)-β-cyclodextrin hydrate [104].

The 3D structures models were added into the structure, which was then fully optimized by semi empirical as PM3, and *ab initio* calculation with Hartree-Fock by using 6-31G(d, p).

37
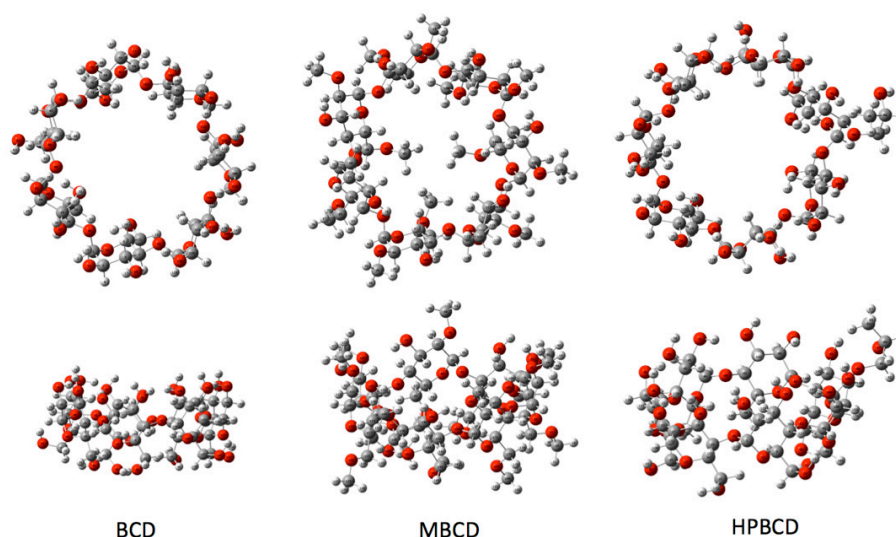
Figure 3.6: The top and front view of all host molecule: BCD, MBCD and HPBCD, all of them were downloaded from CCDF and modified by removing the solution.

3.6.3 Molecular docking simulation (procedure)

AutoDock calculation is performed in 4 steps:

1. Coordinate file preparation: in this step the input file (file.pdb) of ligand and host molecules are extended to pdbqt format. For the pdb format, it contains the coordinate of the molecule. Therefore the pdbqt file includes atomic partial charges, atom types and the torsional degree of freedom.

2. AutoGrid calculation: this is precalculating process which find the atomic affinity potential of each different atom in ligand molecule is docked. The host molecule is enclosed into 3D grid and probe atom, which is placed at each grid point. AutoGrid affinity grids such as electrostatic and desolvation potential are calculated for each type of atom in ligand. The grid will evaluate the energetics of a particular ligand configuration.

3. Docking using AutoDock: AutoDock4.2.6 uses the most efficient method, which call Lamarckian genetic algorithm (LGA) [99] simulated annealing. The calculation will run several times to provide the docked conformations. The calculated energy is show with the number of occurrence or the consistency of the conformation, which are the factors to select the candidate molecules.

4. Analysis using AutoDockTools: AutoDockTools contain the method for analyzing the result from docking. The cluster or the conformation result can be illustrated as the conformation similarity, visualizing conformations, interaction between ligand and host visualization and visualizing the affinity potential which created by AutoGrid.

Table 3.5: The grid box dimension of host molecule set by Autodock program (Number of point).

Inclusion complex with host molecule	Dimension (Number of point)		
	x	y	z
BCD	38	38	20
MBCD	42	38	26
HPBCD	50	38	26

3.6.4 Binding energy analysis

Binding energy is one of the factor to consider whether our host and guest molecules prefer to form the inclusion complex or not. The calculation follows this equation:

$$\Delta E_{binding} = E_{complete} - (E_{host} + E_{guest}) \qquad (3.19)$$

where $E_{complex}$ is the energy of inclusion complex between host and guest; E_{guest} is the energy of guest molecule; and E_{host} is the energy of host molecule. The inclusion complex which illustrates the lowest energy (negative) is the most stable inclusion complex. Therefore, the positive value means that the inclusion complexes are unlikely to form the inclusion complexes. Act as monomer molecule is more stable than to form the inclusion complex.

3.6.5 CBS and BSSE

In quantum mechanic calculations, when we used one-electron basis sets of gaussian functions to ease our computational demand. There is the mathematical imcompleteness in finite basis sets in our calculationas we know as the basis set superposition error (BSSE). We can estimate the basis set imcompleteness by considering the extrapolations of the complete basis set (CBS)

The complete basis set (CBS)

The complete basis set scheme is a series of basis sets designed to extrapolate energies to the infinite basis set limits. CBS limit include higher-order of electron correlation. Hartree-Fock energies were treated by Jasen's scheme [105], which the $\gamma = 9$ and refinment by using Karton and Martin [106]. The energy at the CBS limit (E_{CBS}) is from :

$$E_{\mathrm{CBS}} = E_5 + \frac{E_5 - E_4}{\frac{5}{6}\exp\left[9\left(\sqrt{5}-\sqrt{4}\right)\right]-1} = E_5 + 0.167(E_5 - E_4) \qquad (3.20)$$

where E_4 and E_5 denoting the Hartree-Fock energies calculated in the aug-cc-pVQZ and aug-cc- pV5Z basis sets, respectively [107].

The Basis Set Superposition Error (BSSE)

Basis Set Superposition Error (BSSE), arised from the localized nature of LCAO basis set, is considered to evaluate the interaction energy of the inclusion complexes between two molecules. The error can occur in the calculation of interaction energy between weakly bond (van der Waals or hydrogen bond system). Normally, the previous correction contains artificially lower energy from the high strength of overestimated hydrogen bond. We can estimate the BSSE using Counterpoise Corrections (CP) from Boys *et al.* [108]. The BSSE is estimated as the differences between each monomers using the regular basis and calculated the energy with total basis function set for the molecule of inclusion complex. Follow the

Figure 3.7, we consider fragments A and B as a single atom. At the first step, A and B are apart, each fragment are explained by the basis orbitals centered at each respective atomic nuclei. Then, two atoms interact together, the basis set functions centered at A overlap with center of B. As a result, part of basis set orbitals centered at B is available to describe to A, which provides higher attraction between A and B. For two fragments (A and B), the complex AB interaction energy can be found from the following equation:
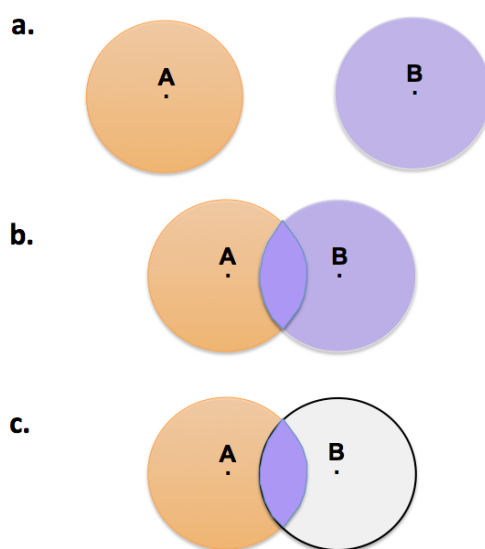
Figure 3.7: Schematic basis set superposition error. (a) A and B are monomers molecule apart from other; (b) basis orbitals overlap when A interact to B; (c) the purple area indicates the part of the basis orbitals centered at B available to describe A.

$$\Delta E_{AB} = E_{AB} - (E_A + E_B) \tag{3.21}$$

where the energy of the complex combining basis of both fragments can be ditated by E_{AB}. On the other hand, E_A and E_B are the fragments energy. The basis set functions on B can improve the fragment A. Therefore, just the basis set refer to each fragment was used in the computation of the separated fragment (A or B). For example, if we calculate the fragment

A, the ghost basis of fragment B can serve to counterbalance basis B effect on fragment A in the calculation of AB inclusion complex. Thus, interaction energy can be performed as counterpoise-corrected interaction energy.

$$\Delta E_{AB}^{CP} = E_{AB} - E_A^{CP} - E_B^{CP} \tag{3.22}$$

Here, E_A^{CP} is the counterpoise-correction fragment A energy in full basis set of inclusion complex AB including the ghost functions located with system B. The interaction energy can be derived from the following equation, similary to the counterpoise correction.

$$\Delta E_{corr}^{CP} = \Delta E_{AB}^{CP} - \Delta E_{AB}$$
$$\Delta E_{corr}^{CP} = (E_A - E_A^{CP}) + (E_B - E_B^{CP}) \tag{3.23}$$

In fact, the counterpoise correction is consistency presented in positive value because $E_A > E_A^{CP}$ and $E_B > E_B^{CP}$ for variation wave functions. For no variation wave functions, the correction is negative. BSSE consideration is depending on the type of interactions, but it seems to be crucial for weakly bond as van der Waals bond than the molecules with chemically bounded [109].

Chapter 4

Results and Discussions

In this chapter, the results are presented following the procedure in the research methodology section. First, we will start from the geometry optimization of the structure, AutoDocking, binding energy calculation and the calculation of electronic properties. Then, all results are discussion in this section. Finally, the computation cost of different methods are shown in the last section.

4.1 Geometry Optimization

The geometry optimization can be divided into 2 phases. The first step starts from the geometry optimization of monomers molecule including plumbagin and all the host molecules (BCD, MBCD and HPBCD). Subsequently, the AutoDock program is used to predict the possible conformation of the inclusion complexes. After we recognize the possible conformations, we begin the inclusion complex geometry optimization.

4.1.1 Monomers optimization

It is important to pre-optimize the system by using semi-empirical methods (like PM3 before submitting to *ab initio* calculations). The PM3 results may provide at unreasonable minima, so it might be useful to continue the calculation with *ab initio* method. For cyclodextrins system, the semi-empirical have been studied, and the results have been shown that, semi-empirical (PM3, PM6 and AM1) is reasonable for cyclodextrins system [96]-[110]. However, for ground state geometry optimization, geometries optimized with B3LYP method and the 6-31G(*d*) basis set is a recommended model for reliable prediction typically benefit from an accurate geometry and large basis set as shown in Figure 4.4.

4.1.2 Inclusion complex molecule

After monomer structures optimization of each basic sets as shown in Figure 4.4, we performed the molecular docking between the ligand and host. The possible conformations were presented after the molecular docking, and two types of conformations were found in
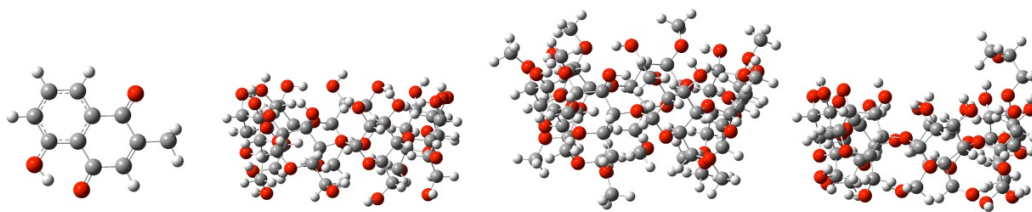
Figure 4.1: Monomer optimized structures of all host and guest with DFT/B3LYP/6-31G(*d*) basis set.

most of the cases of each basic set as shown in Figure 4.3. The first conformation is UP, and the methyl group in plumbagin molecule point up in the same direction with the wider rim of the truncated cone of BCDs molecule. On the other hand, the DOWN conformation is in the opposite direction.

4.2 AutoDocking Results

Molecular Docking result of PM6 calculations are illustrated as the possible conformations, which can occur as shown in Figure 4.2. The four possible clusters of the inclusion complex between BCD and plumbagin are displayed. The possibility to form cluster 1 is equal to 20%, cluster 2 for 46%, cluster 3 for 33%, and cluster 4 for 1%.

Cluster 1 (20%)	Cluster 2 (46%)	Cluster 3 (33%)	Cluster 4 (1%)
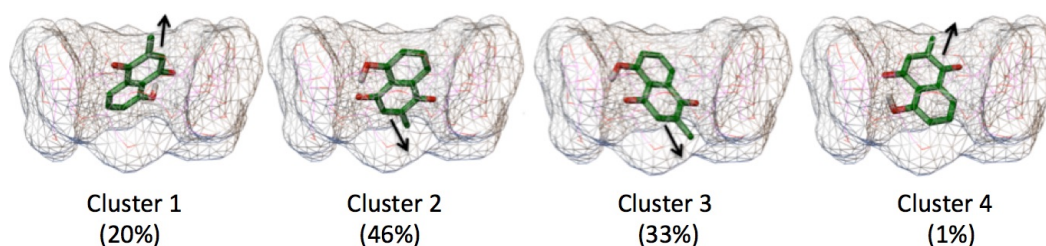
Figure 4.2: Docking results of the inclusion complex between BCD and plumbagin, the percentage of occurrences are given in parentheses.

All four clusters can be grouped into 2 types according to the direction of the arrows. The conformation-I illustrates the inclusion complex in which the methyl group of the plumbagin is pointing up to the wider rim of the truncated cone. The conformation-II is shown in the different direction as shown in Figure 4.3. Table 3.5 shows the molecular docking results of PM3, PM6 and DFT/B3LYP/6-31G(*d*) basis set calculation. All BCDs from PM3 calculation are displayed, while conformation-I provides the highest percentage of occurrence. On the other hand, conformation-II provides the lowest energy. In PM6, BCD inclusion complex illustrates 5 clusters and all the clusters are conformation-I. HPBCD is also similar to BCD, that the 100% occurrences are conformation-I. For MBCD, cluster1 is the conformation-I, with the 87% occurrence, while the remaining 13% is conformation-II.

In DFT/B3LYP/6-31G(*d*), the conformation-I for BCD gives the lowest energy. Therefore, MBCD and HPBCD express the conformation-II with the lowest energy. Out of all
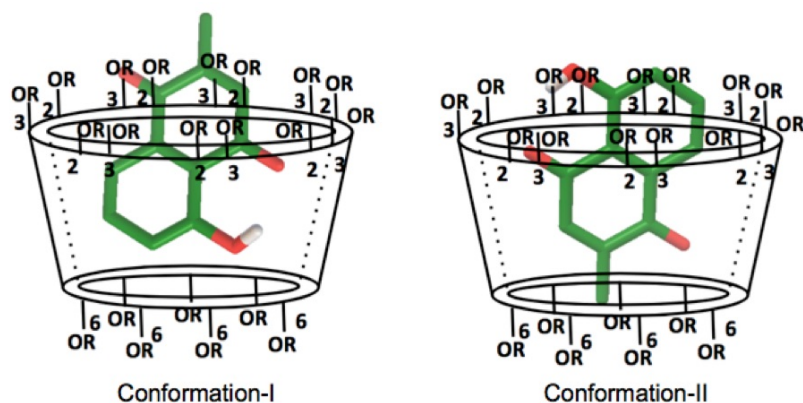
Figure 4.3: Two main possible conformations from docking calculation of inclusion complex. Conformation-I is "UP" which the methyl-group point up to the wider rim of the truncated cone and conformation-II is "DOWN", which the methyl-group of plumbagin molecule point in the opposite side.

the cases, the highest percentage of occurrence is conformation-II. Thus, for the first state, the conformation-II is the most preferable conformation for BCDs and plumbagin inclusion complex. Comparison to semi-empirical PM3 and PM3 with PCM basis set, conformation-I is the highest percentage of occurrence. PM6's result also expresses similar to PM3, which the conformation-I showed the highest percentage.

The free energy of binding ($\Delta G_{\text{binding}}$) are estimation is calculated from ΔH - $T\Delta S$, where ΔH is the enthalpy, while ΔS presented the entropy and the calculation temperature is at 298.15K. Following the Table 4.1 - 4.4, all of binding energy is negative value, which means all of the inclusion complexes are suitable to form. MBCD expresses the lowest negative sign. The same results with the DFT/B3LYP/6-31G(d) are shown in Table 4.4. K_i is the inhibition or dissociation constant calculated from the free binding energy. If the value of K_i is lower, the ligand and host are preferred to bind more. BCD illustrates the highest value while MBCD shows the lowest than the others for PM6 and B3LYP/6-31G(d).

4.3 Binding Energy Calculation

In this part, we catagories the results into two phases. The first phase is the primary calculation from semi-empirical calculation. Subsequently, the second phase, DFT hybrid functionals and dispersion correction functionals were performed.

4.3.1 Semi-empirical

After docking calculation, the result illustrates that two types of conformations can be the candidate of plumbagin and BCDs inclusion complex. Two types of conformations from each hosts were performed the geometry optimization with PM3, PM6 and PM7 methods. From Figure 4.5, all of the calculations illustrate negative value in binding energy, which

Table 4.1: Molecular docking calculation results of three host; BCD, MBCD and HPBCD with plumbagin by using PM3 method.

| Compound | Cluster | Conformation | %Frequency | E_{binding} (kcal/mol) | | K_i (micromolar) |
				lowest	mean	
BCD	1	I	100	-5.39	-5.37	116.36 ± 3.64
MBCD	1	II	14	-5.43	-5.43	106.75 ± 1.39
	2	I	79	-5.43	-5.42	106.71 ± 1.23
	3	II	7	-5.41	-5.40	107.43 ± 1.09
HPBCD	1	II	7	-5.03	-5.01	214.65 ± 5.66
	2	I	71	-5.02	-5.01	216.52 ± 8.48
	3	I	9	-5.00	-4.98	216.25 ± 7.22
	4	I	11	-4.99	-4.98	219.59 ± 11.66
	5	I	2	-4.92	-4.92	213.98 ± 9.88

Table 4.2: Molecular docking calculation results of three host; BCD, MBCD and HPBCD with plumbagin by using PM6 method.

| Compound | Cluster | Conformation | %Frequency | E_{binding} (kcal/mol) | | K_i (micromolar) |
				lowest	mean	
BCD	1	I	86	-5.12	-5.09	189.44 ± 15.15
	2	I	5	-5.08	-5.07	183.65 ± 5.56
	3	I	4	-4.99	-4.99	193.34 ± 25.68
	4	I	3	-4.96	-4.96	182.60 ± 1.14
	5	I	2	-4.96	-4.96	180.25 ± 3.25
MBCD	1	I	87	-5.50	-5.49	94.63 ± 2.15
	2	II	13	-5.46	-5.46	106.71 ± 1.23
HPBCD	1	I	100	-5.42	-5.40	109.78 ± 5.48

Table 4.3: Molecular docking calculation results of three host; BCD, MBCD and HPBCD with plumbagin by using PM7 method.

| Compound | Cluster | Conformation | %Frequency | E_{binding} (kcal/mol) | | K_i (micromolar) |
				lowest	mean	
BCD	1	II	36	-5.06	-4.97	195.98 ± 12.43
	2	I	9	-5.04	-5.00	202.50 ± 6.76
	3	I	55	-5.01	-4.99	212.29 ± 11.31
MBCD	1	I	100	-5.45	-5.44	100.94 ± 0.79
HPBCD	1	II	89	-5.84	-5.83	52.27 ± 4.23
	2	I	7	-5.74	-5.72	61.99 ± 7.32
	3	II	4	-5.66	-5.65	70.46 ± 4.15

Table 4.4: Molecular docking calculation results of three host; BCD, MBCD and HPBCD with plumbagin by using DFT/B3LYP/6-31G(d).

Compound	Cluster	Conformation	%Frequency	$E_{binding}$ (kcal/mol) lowest	mean	K_i (micromolar)
BCD	1	I	20	-4.91	-4.90	260.59 ± 9.34
	2	II	46	-4.90	-4.89	261.50 ± 4.48
	3	II	33	-4.88	-4.88	260.29 ± 6.04
	4	I	1	-4.83	-4.83	261.07 ± 0.00
MBCD	1	I	87	-5.67	-5.65	74.29 ± 4.94
	2	II	12	-5.57	-5.56	75.12 ± 5.43
	3	II	1	-5.51	-5.51	70.54 ± 0.00
HPBCD	1	I	99	-5.21	-5.20	154.07 ± 5.79
	2	II	1	-5.10	-5.10	154.88 ± 0.00
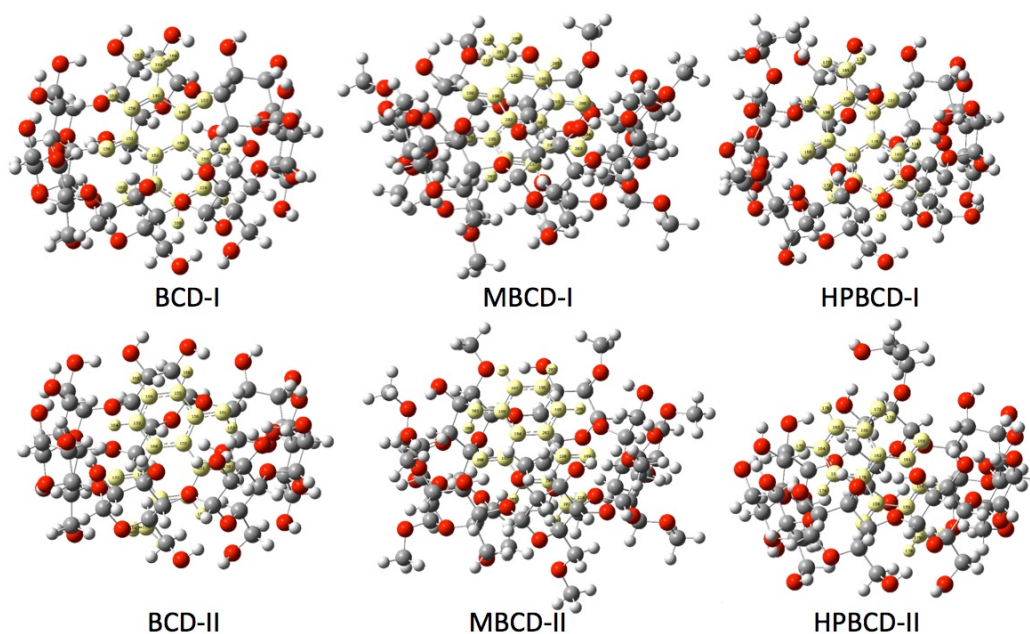
Figure 4.4: Optimized structures after docking calculation, the candidate structures were selected from the lowest energy and the highest percentage of occurence.

means that all of the conformations prefer to form the inclusion complex. The results from PM3, PM6 and PM7 calculation is presented respectively. Firstly, PM3 are in the following order:

MBCD-II < HPBCD-I < HPBCD-II < MBCD-I < BCD-I < BCD-II

For PM6 result, the binding energy are in the following order:

BCD-II < BCD-I < MBCD-I < HPBCD-I < MBCD-II < HPBCD-II.

For PM7 are in the following order:

HPBCD-II < MBCD-II < HPBCD-II < BCD-II < MBCD-I < BCD-I

PM3 and PM6 provide the same range of binding energy. The PM7 method can improve
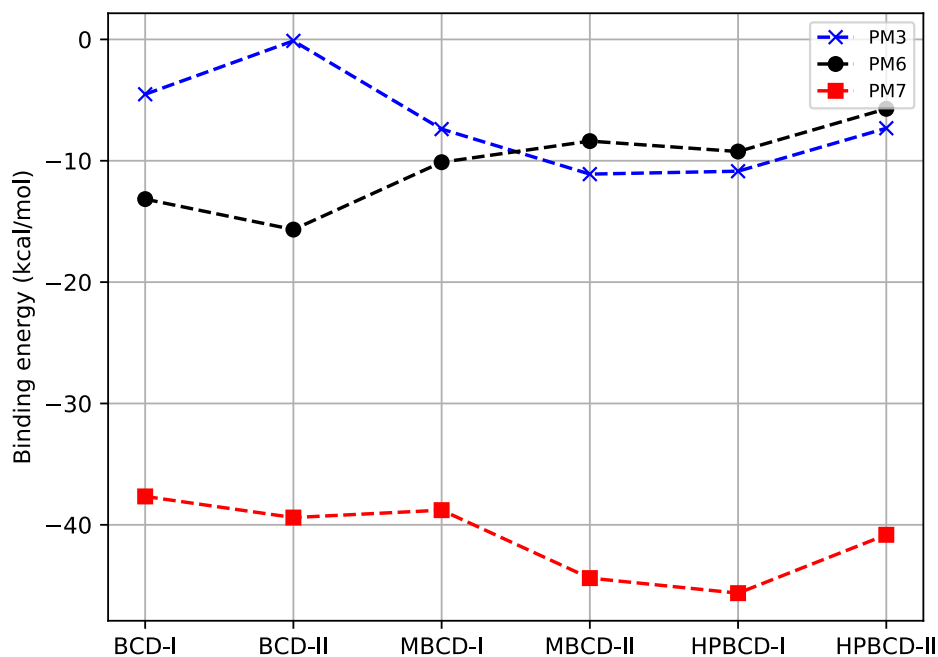
Figure 4.5: Binding energy of six conformations by semi-empirical methods, including PM3, PM6 and PM7. PM7 provides the similar trend to PM3, but the binding energy illustrates lower than PM3 and PM6.

some properties such as the heats of formation (height of the reaction barriers for reactions) and include them into dispersion interaction and hydrogen bonding in the parametrization [61], which should be suitable for the description of non-covalent interactions. On the other hand, there are some limitations of this method including large error for the non-covalent interaction energy [59]. PM3 and PM7 provide the similar trend in the different range of binding energy, but PM6 does not. Three methods illustrate the different candidate conformation. PM3 shows MBCD-II, while PM6 represents BCD-II, and PM7 suggestss that HPBCD-I is the candidated conformation. To specified the force, the factor affecting

the binding energy of each conformation, we consider the interactions between host and guest of the complexation. The intermolecular interactions between host-guest include, hydrogen bond interaction, C-H bond interaction and hydrophobic force. The number of bond of each methods are counted and shown in Table 4.5.

To confirm with the previous studies, in PM7's prediction is overbinding, we plot the graph as shown in Figure 4.6. The graph represents the average number of intermolecular bond of each functional of conformation. PM6 provides the lowest average intermolecular bond length comparing to PM3 and PM7. PM3 provides the highest of average intermolecular bond length. The total average bond length of PM3 is 2.57 Å, PM6 with 2.33 Å, and PM7

Table 4.5: Number of intermolecular bonding, consisting of hydrogen bond, C-H bond and hydrophoblic interaction, for each case. Criteria of bonding detection from Discovery Studio 4.0 Visualizer program. The required Hydrogen bond distance criterion is 2.5 Å.

Method	BCD-I	BCD-II	MBCD-I	MBCD-II	HPBCD-I	HPBCD-II
PM3	3	6	3	2	1	3
PM6	5	8	7	7	7	7
PM7	6	7	9	8	6	10

with 2.50 Å. PM6 provides the shortest average bond length than others. PM7 expresses the longer averege bond length, but the variation of the result is reduce.

After the analysis, it is found that the similar discussion using the above plot as the preceding one does not work here. Since, not only the length, but also the number of bond affect the binding energy, the type of bond is also one of the factor. As in the Chapter 2.3, the interaction between host-guest of hydrogen bond.
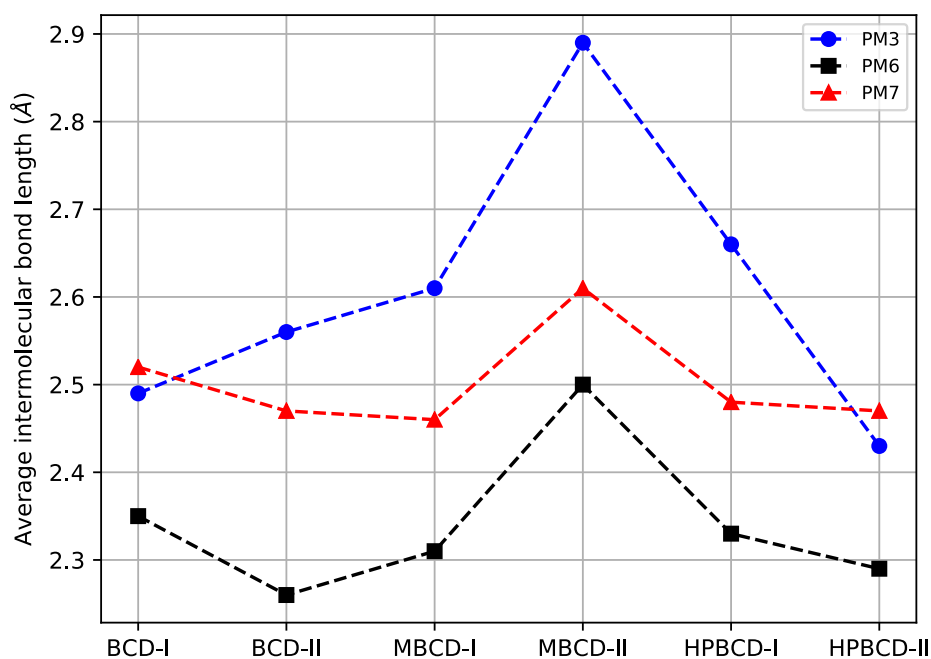
Figure 4.6: The average intermolecular bond length between host and guest using semi-empirical method (PM3, PM6 and PM7), the intermolecular bonds were detected from Discovery Studio 4.0 visualizer program. PM6 provides the lowest average intermolecular bond length.

We have studied the plumbagin and BCDs inclusion complex in two different conditions, which including gas and in water solusion. The result of two different phases are represented as the following:

Plumbagin-BCD inclusion complex

Up and down conformations of plumbagin-BCD inclusion complex can be formed both in gas phase and in aqueous phase, as shown in Figure 4.7. In gas phase by PM6 calculations (PM6/Gas), BCD-I and BCD-II form one hydrogen bond between the plumbagin's hydroxyl group with one linked oxygen atom between two glucose units, with the distance of 2.77 Å and 1.96 Å, respectively. These hydrogen bonds also occur in PM7/Gas calculations with the distance of 2.92 Å and 2.61 Å for BCD-I and BCD-II, respectively. The shorter distance of hydrogen bonds, the stronger of molecular interactions, which also indicated by the E values. Therefore BCD-II is the favorable conformation in gas phase. The calculations suggest that both BCD-I and BCD-II conformations are possible to occur in aqueous environment. Two hydrogen bonds are occurred between plumbagin's hydroxyl group with one of linked oxygen atom of two glucose units and with the hydrogen atom at C6 position of BCD molecules. A shorter hydrogen bond distance in BCD-I conformation influence to the stronger host-guest molecular interaction in PCM models.

Method	Gas		PCM	
	BCD-I	BCD-II	BCD-I	BCD-II
PM3				
PM6				
PM7				
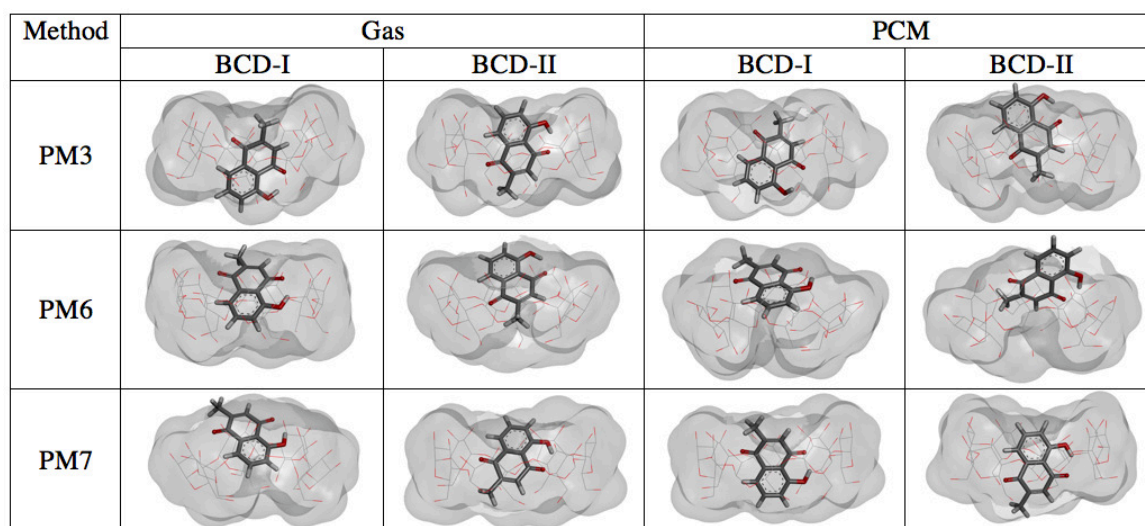
Figure 4.7: BCD inclusion complex structures, which optimized in gas and water solution phase. Plumbagin is illustrated as stick models. BCD molecules are as line model with van der Waals surface with the probe radius 1.4 Å.

Plumbagin-MBCD inclusion complex

Due to the presence of methyl group at the primary hydroxyl group of BCD (C6-CH_2OCH_3), the entrance of plumbagin at the narrow side of MBCD is difficult. According to the steric and electronic hindrances, plumbagin can enter MBCD at the wide side and can form the inclusion complex MBCD-I and MBCD-II conformations, as shown in Figure 4.8. Only MBCD-I conformations from PM6/Gas and PM7/Gas calculations, have one ordinary hydrogen bond which occurs between plumbagin's hydroxyl group with the ether-like anomeric

oxygen atom of MBCD. In PM6/Gas, MBCD-I is a favorable conformation, due to it has a hydrogen bond between host-guest with the distance 2.37 Å. For PM7/Gas, MBCD-II is preferred due to the hydrophobic interaction between host-guest with the lower in $E = 5.60$ kcal/mol than MBCD-I. Even though no H-bond founding between plumbagin and MBCD inclusion complex in water environment, but the complexes are stabilized by their hydrophobic interactions which indicated by their binding energy (E) values. The presence of the methyl group at C2-OCH$_3$ of all glucose units in MBCD affect the geometry and the interaction of its inclusion complexed with plumbagin molecule. The plumbagin molecules are located near the wide side, both in MBCD-I and MBCD-II inclusion complex conformations.

Method	Gas		PCM	
	MBCD-I	MBCD-II	MBCD-I	MBCD-II
PM3				
PM6				
PM7				
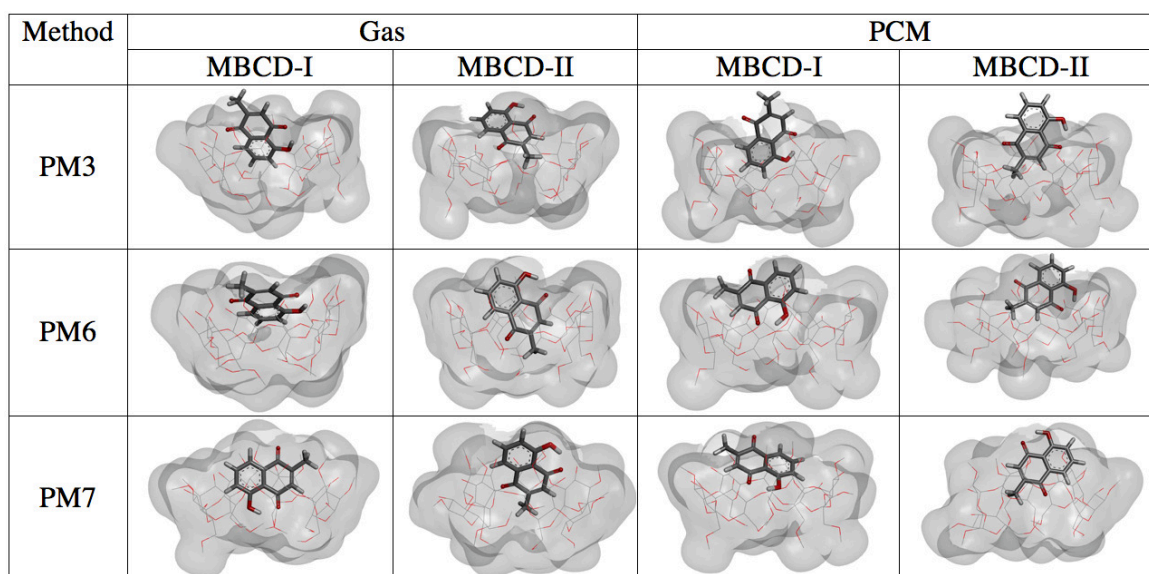
Figure 4.8: MBCD inclusion complex structures, which fully optimized in gas and water solution phase. Plumbagin is presented as stick models. MBCD are presented as line model with van der Waals surface with the probe radius 1.4 Å.

Plumbagin-HPBCD inclusion complex

The presence of 2-O-((S)-2-hydroxypropyl) group at one of the glucose unit in HPBCD enlarge the width of the wide side of its truncated cone and break its intra molecular H-bonds network, which more welcome the entrance of plumbagin molecule than the narrow side of HPBCD. According to the steric and electronic hindrances, plumbagin can enter HPBCD at the wide side and can form the inclusion complex, both in HPBCD-I and HPBCD-II conformations, as shown in Figure 4.9. PM6 calculations prefer the formation of HPBCD-I with the

E different 3.38 to 3.52 kcal/mol lower than HPBCD-II, for plumbagin-HPBCD inclusion complex, both in gas and in aqueous phases. This may explain by the electronic interaction between the plumbagin's methyl group with the oxygen atoms of the hydroxyl groups

around the wide rim of HPBCD, in HPBCD-I configurations. The H-bond between hydrogen atom of plumbagin's hydroxy group and ether-like anomeric oxygen atom of HPBCD was formed in all complexes conformations optimized by PM6 methods. In PM7 methods, the inclusion complex of plumbagin and HPBCD in both conformations are stabilized, both in gas phase and in water environment. PM7 calculations indicate the favorable formation of HPBCD-I with binding energy 4.81 kcal/mol lower than HPBCD-II. Nevertheless in water environment calculations, PM7/PCM, indicate HPBCD-II is much more favorable with binding energy 9.54 kcal/mol lower than HPBCD-I. In HPBCD-II optimized by PM7/PCM method, the methyl part of the hydroxypropyl group substituent fall into its cavity due to the hydrophobic interaction with plumbagin's hydroxyl phenolic part, and push the plumbagin molecule locate deeper inside its cavity.

| Method	Gas		PCM	
	HPBCD-I	HPBCD-II	HPBCD-I	HPBCD-II
PM3				
PM6				
PM7				
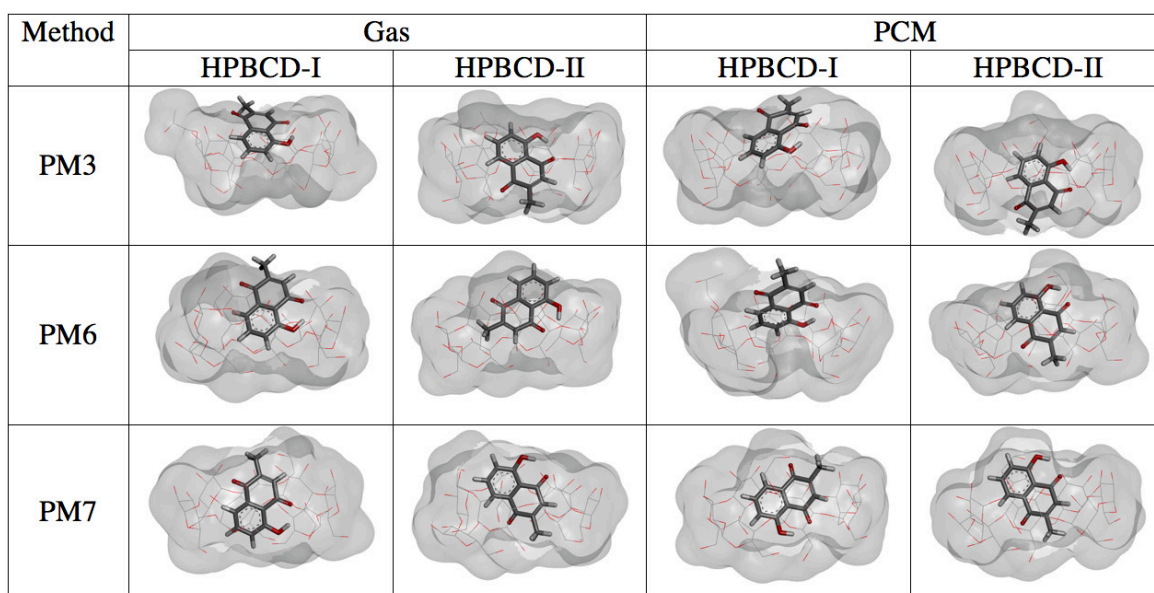
Figure 4.9: HPBCD inclusion complex structures, which fully optimized in gas and water solution phase. Plumbagin is presented as stick models. HPBCD are presented as line model with van der Waals surface with the probe radius 1.4 Å.

The semi-empirical PM6 and PM7 methods were employing to study the 1:1 host-guest complexation of plumbagin with BCD, MBCD and HPBCD, both in gas and in aqueous phases. The binding energy values of each systems obtained by PM7 methods are significantly lower than PM6 methods, though the geometry of the complexes are not much differ. Our results indicate the insertion pathway of plumbagin molecule into BCDs' cavity from the wide side of truncated cone with two possible orientations. The intermolecular hydrogen bonds and hydrophobic interactions play an important role in the complexation process of the plumbagin with BCDs.

Table 4.6: Binding energy (kcal/mol) result between two different basis sets B3LYP6-31G(d) with B3LYP6-31++G(d, p) with the raw and corrected result from BSSE correction of all configuration.

Configuration	6-31G(d)		6-31++G(d, p)	
	raw	corrected	raw	corrected
BCD-I	-8.89	0.65	-3.40	1.02
BCD-II	-13.93	-1.87	-4.27	0.65
MBCD-I	-6.79	2.75	-2.24	1.25
MBCD-II	-6.67	-0.77	-6.84	-4.86
HPBCD-I	-5.00	3.07	-4.60	-0.87
HPBCD-II	-6.12	1.89	-1.94	3.11

4.3.2 Conventional DFT functional

The hybrid functional, B3LYP is selected for the computation. Since many studies have shown that this functionals provide better in geometry optimization structure, as a result the final structure after performed geometry optimization is uniform. As a result, it is reliability to decribe the intramolecular. First step, the smaller 6-31G(d) basis set was chosen according to the other studied [87]. Afterward, for more accuracy the 6-31++G(d, p) was performed. In DFT/B3LYP/6-31G(d), the polarization was considered, and d-primatives has been added to other atom (except the hydrogen atom). DFT/B3LYP/6-31++G(d, p) is larger basis set in 6-31++G(d, p), this basis set considers full dispersion functional and polarization. Four out of six conformations illustrate positive value. Two conformations provide negative value. MBCD-II gives the lowest in binding energy. After observing the last conformation, we found that the guest molecule float out from the host. That means in B3LYP/6-31++G(d, p) basis set, our host and guest are unlikely to form the inclusion complex.

Comparison between two different basis sets

Comparison between two different basis sets between 6-31G(d) and 6-31++G(d, p) basis sets. Table 4.6 represent the raw and corrected binding energy results of all configuration. Comparison between two basis, two basis express the different lowest point of binding. The lowest binding energy of 6-31G(d) is BCD-II and 6-31++G(d, p) is MBCD-II. The lowest energy between raw and corrected data are the same. Two basis sets provide the different gap between raw and corrected of binding energy. DFT/B3LYP/6-31++G(d, p) shows the smaller gap, which means the % BSSE correct of larger basis set is less.

4.3.3 DFT dispersion correction functionals

The hybrid (B3LYP) functional, the most popular and commonly used for the organic molecular system, cannot explain the intermolecular interaction well. Eventhough, the intermolec-
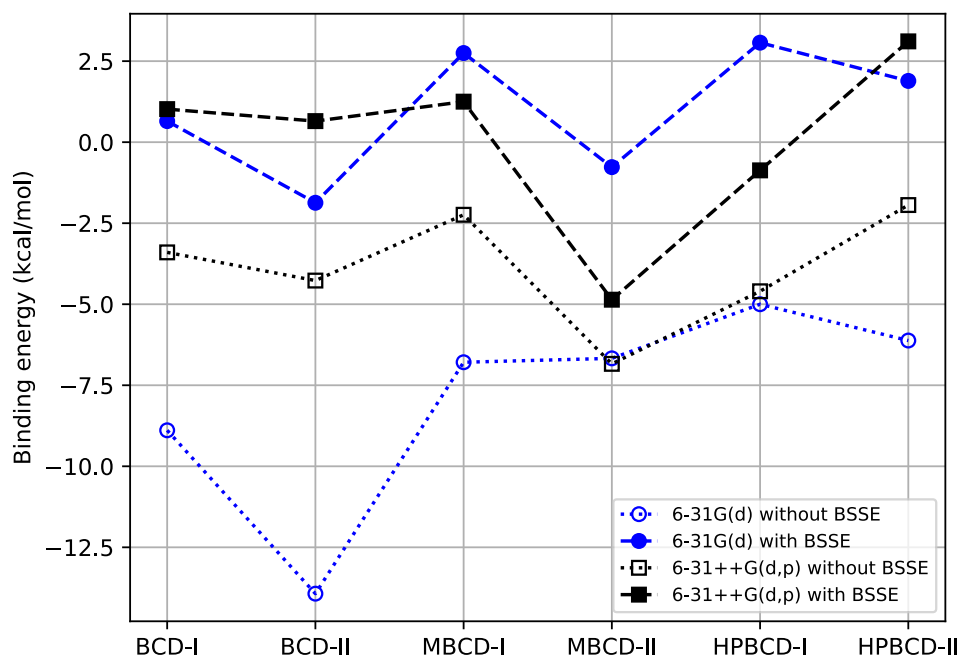
Figure 4.10: Comparison between two different basis sets of B3LYP6-31G(*d*) with B3LYP6-31++G(*d*, *p*). B3LYP6-31++G(*d*, *p*) represents the smaller gap between the raw binding and corrected results.

ular interactions is very important for many systems. Therefore, many of dispersion correction functionals have been developed. To improve the efficiency to capture the interaction between two molecule in organic system, non-covalent interaction such as dispersion or van der Waals and hydrogen bond play in the important role. Six functionals are chosen and performed the calculation. For our target system, each of the structures was optimized by each functional. The final strucutres of each functionals are different. Only B3LYP provides the positive value in binding energy, while others functionals illustrate the negative value. Other functionals with DFT-GD correction show the lower range of binding energy between -33.23 to -15.04 kcal/mol. M06-2X functional also provide low binding energy in the range between -21.61 to -13.51 kcal/mol. B3LYP provide the highest binding energy. The conventional functional is unable to discribe the long-range or the intermolecular interaction correctly. After considering CAM-B3LYP, we consider the interaction energy of our system in two terms. The first term is the short-range interaction calculated from 0.19HF + 0.81B88. The other term is the long-range interaction from 0.65HF + 0.35B88. This functionals can capture further range of interaction from the higher fraction of HF. Therefore the better spatial overlap of distance donor and acceptor orbital of the host-guest are represented [111]. As a result, the lower binding energy are obtained. The trend of each conformation is similar to B3LYP binding energy decrease. The candidate conformation is MBCD-II, which is the

same conformation with B3LYP functional. For B3LYP-GD3 or B3LYP-GD3 functional, this functional includes vdW interaction with default parameters for GGA-PBE functional. The C_6 or the dispersion coefficient is from TDDFT for hydrides, and modified by coordination number [72]. The C_6 can capture the intermolecular interaction part. For all B3LYP with DFT-GD3, the binding energy decrease to the range of -25.46 to -33.23 kcal/mol. Trend of binding energy is different from B3LYP, that might be from the different final optimized structures of B3LYP. As a result, the candidate conformation is changed from MBCD-II to HPBCD-II.
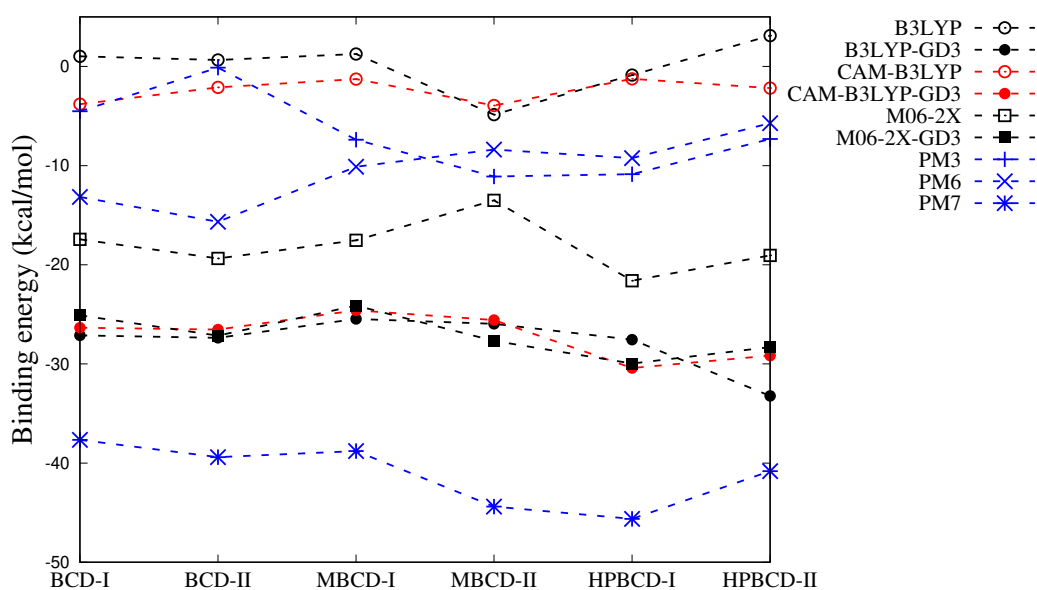
Figure 4.11: Calculation binding energy using conventional (B3LYP) and dispersion corrected functionals.

The binding energy results of M06-2X and M06-2X-GD3 provide similar trend, but M06-2X with DFT-GD3 correction gives the lower binding energy. Two functionals express the same candidate conformation, which is HPBCD-I. M06-2X is a high non-locality with double amount of nonlocal exchange (global hybrid functional contains 54% HF exchange). The higher percentage of HF helps M06-2X to capture the long-range interaction part, that related to the higher negative value of binding energy. Otherwise, the effect from damping functional of DFT-GD3 affect the M06-2X-GD3 functional resulting in lower number of binding energy.

Table 4.7 represents the deviation value from the average number of geometry optimized energy to make the table is easily to compare between each results. For the DEV$_{\text{comp}}$ column, the value deviate from the average value, which we divide the geometry optimized energy into three groups following the host molecules. The first group is BCD complexes, which have the average number of geometry optimized energy -3,089,919.95 kcal/mol. Next group is MBCD complexes, the average number of geometry optimized energy -3,435,058.86

kcal/mol. The last group is HPBCD complexes, the average number of geometry optimized energy -3,211,091.48 kcal/mol.

For DEV$_{hosts}$, we also groups into three groups as the inclusion complex molecules. The average number of geometry optimized energy for BCD, MBCD and HPBCD -2,682,323.08, -3,027,462.65 and -2,803,494.05 kcal/mol respectively. For DEV$_{guest}$, the average number of geometry optimized energy -407,576.43 kcal/mol. According to Table 4.7 , considering between the $E_{binding}$ and $E_{corrected}$. $E_{binding}$ is the number which is from the calculation follow Equation 3.1, and $E_{corrected}$ is the number after corrected with BSSE correction. If we do not consider the incompleteness from basis set, the candidate molecule that we selectted will be different. For example, in CAMB3LYP, the $E_{binding}$ represents BCD is the candidate molecule. On the other hand, $E_{corrected}$ illustrates MBCD is the candidate host. The other functional calculations also provide the different results.

4.3.4   Percentage of BSSE correction

Figure 4.12, the percentage of BSSE corrections were ploted and compared between each basis set. The different legends means each conformations. The results show, B3LYP provides the scatter data, the data vary between 25 to 270 %. For CAM-B3LYP, the % BSSE corrections are in the range between 45 to 80 %, which is high number, but the scatter of data reduce. M06-2x functional illustrate the less number of %BSSE corrections and scatter of the data. Finally the functionals which included DFT-GD3 (B3LYP-GD3, M06-2x-GD3 and CAM-B3LYP-GD3) represent the less scatter of the result, in the same way with lower number of % BSSE corrections.
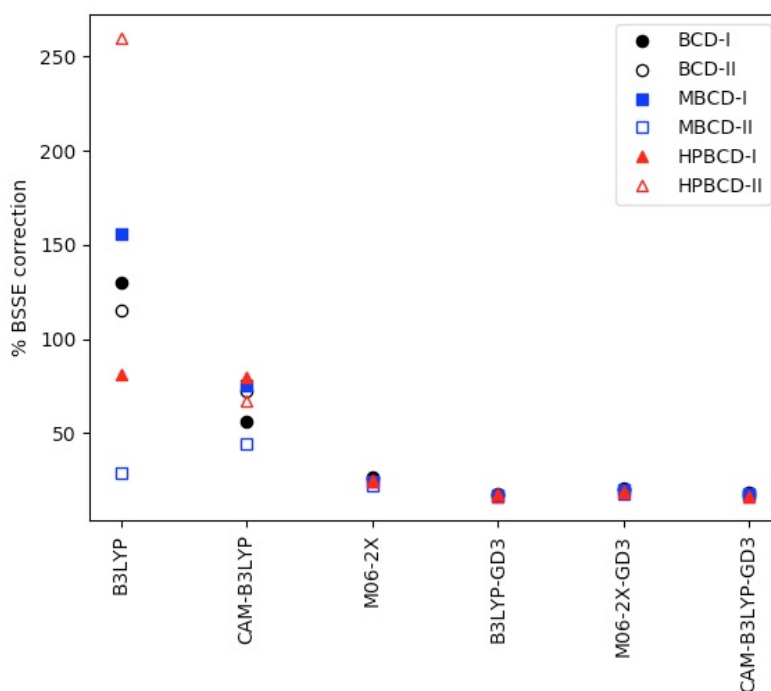

Figure 4.12: Fraction of BSSE corrections.

% BSSE corrections depends on many factors, for instance the basis set and from Klopper *et al.* [78], presents the increase in BSSE may be from the decreasing of inter monomer distance. That can be related from the non-covelent bondings of the system, the distance between dependences of electrostatic, exchange and the dispersion term [112] Our system, we consided only one basis set (6-31++G(d, p)). Therefore, the main reason may cause from non-covalent bonds which related to each functionals can capture them or not. As the previous section, B3LYP cannot capture long-range interaction well comparing to M06-2X and other case which add dispersion correction term. So, the intemolecular interaction between host-guest from B3LYP calculation might be shorter and may cause the higher number of %BSSE. M06-2X and other functionals with dispersion correction can capture the long-range interaction. That might affect to the less different in %BSSE corrections.

4.4   Computational Cost

We compare the computational cost between the different methods including semi-empirical (PM3, PM6, and PM7) and DFT (CAM-B3LYP, M06-2X, B3LYP-GD3, M06-2X-GD3 and CAM- B3LYP-GD3). Figure 13 illustrates the elapsed time comparison in second between two mains different methods. The inclusion complex BCD with plumbagin (UP conformation) was performed single point calculation using various methods and functionals with 12 cores run. A significantly difference of elapsed time between semi-empirical (7-10 [sec.]) and DFT (12,500-30,000 [sec.]). Parameterization method can solve with time consuming problem effectively. Then, we plot these two methods separately as shown in Figure 4.13.

Figure 4.13 (left) shows the comparison of semi-empirical method using elapsed time, and result in PM6 > PM7 > PM3, respectively. PM3 provides the lowest in computational time, that might be from the PM3 considers 800 reference data sets. On the other hand, PM6 and PM7 consider 9,000 reference data sets, which may cost more computational resource than PM3 [54].

For DFT calculation (right), the calculations take longer time. The hybrid conventional XC functional, B3LYP consumes almost 15,000 [sec.], however for M06-2X functional which consider the empirical fitting data or meta-generalized gradient-approximations (hybrid meta-GGAs) [69] consumes more computational time. Time consuming might be from the higher percentage of Hartree-Fock (54%) gain the time. For CAM-B3LYP correction, the long-range mechanism is used to explain the dispersion force part. This correction also contains higher percentage of Hartree-Fock in the long-range, which consume the higher number of computational cost [72]. For DFT-GD3 dispersion functional correction, the time decreased 14.37% from B3LYP. Similar to the CAM correction, the computational time before adding DFT-GD3 correction is 29,577 [sec.], while the computational time after using DFT-GD3 is 17,466 [sec.] As a result, the computational time can be reduced by 40.95%. On the contrary, the M06-2X functional calculation provides higher computational time after
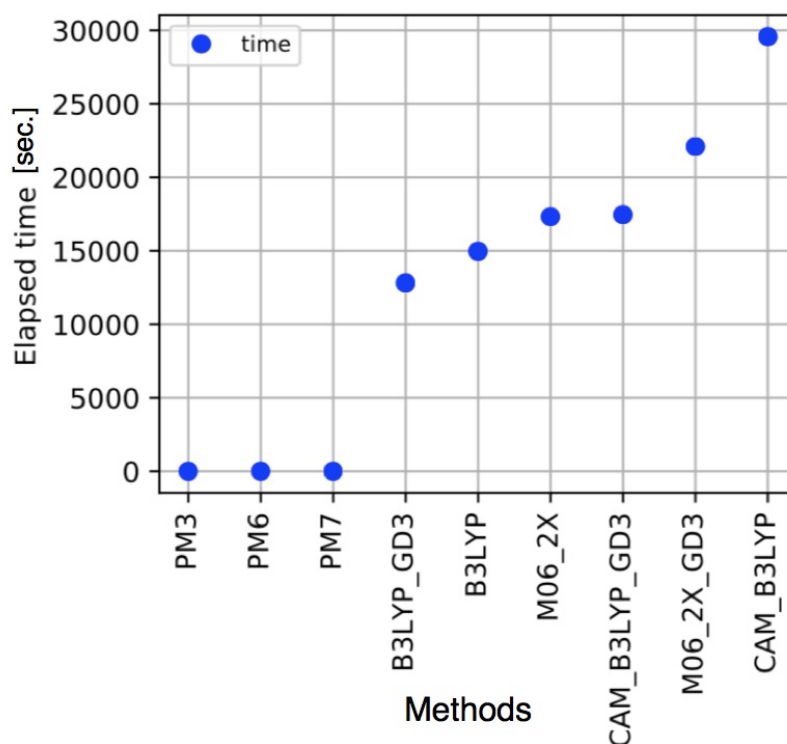
Figure 4.13: Elapsed time of all calculations include semi-empirical (PM3, PM6, and PM7) and five different functionals of DFT calculation of BCD-I conformation with single point run.

performed DFT-GD3, while previously the computed time is 17,331.1 [sec.] After correction by DFT-GD3, the number gaining by 27.52%.

Follow the statement in section 3.4.1, DFT functionals, which DFT-GD3 commonly, the overall of DFT-GD3 energy can be derived from the following equation 3.16, which means the results from this DFT-GD3 correction must be added the E_{disp} term from the conventional DFT XC functional. Computational cost also must be included the extra term. But the result of B3LYP and CAM-B3LYP with DFT-GD3 provided the unexpected result.

So we have continued studied the relationship between number of core and the speed of each method. We found that the different of XC functional provide some unalike in speed. For semi-empirical, PM7 calculation is selected and the runtime is extremely fast, so the input transformation between each core might take more time than finishing by one core. In this case, the size of job is tiny, so we cannot observe the number of core affecting the computational time. Thus, we performed further consideration on the PCM calculation of PM7, that took longer simulation time as shown in Figure 16. The running speed are compared with number of cores. The red dash line is the ideal or the expectation value, hence, if we increase number of core to 10 cores the speed will be increased 10 times. The blue line is the speed of PM7 results, and if we perform 10 cores calculation the speed will start to drop. Subsequently, increasing number of cores to 20 and 48 cores, the speed is steady. Finally, the speed is dropping for 60 cores. Thus, the optimal cores for PM7
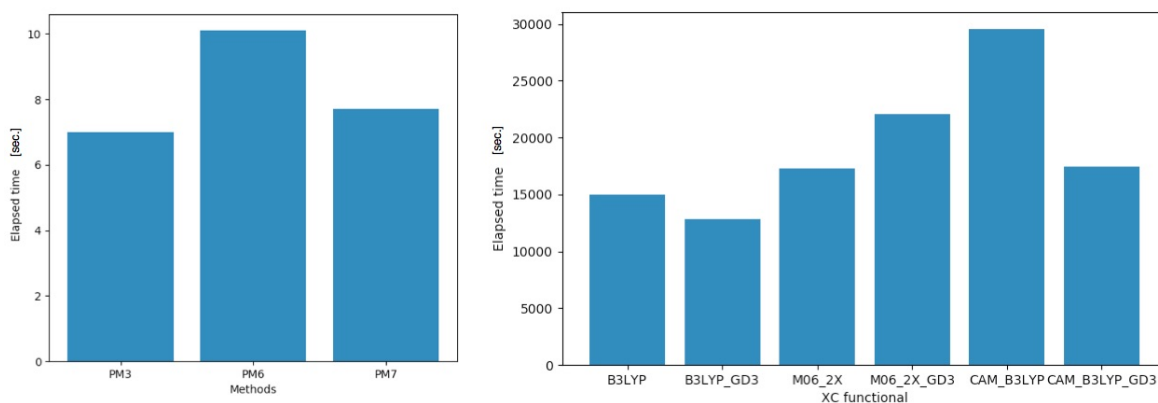
Figure 4.14: Left figure is illustrated the different types of semi-empirical method, and right is figure represented the different functionals calculation of DFT calculation. The elapsed time in second is used for comparison between the different calculations.

calculation is 10 cores. As a result, if we add more than 10 cores, it is insignificant for the calculation speed.
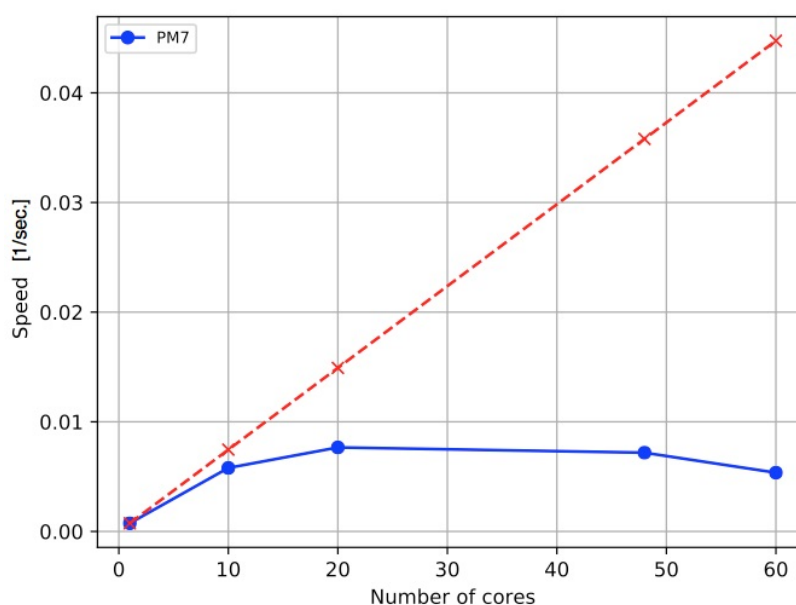
Figure 4.15: The comparison between speed and number of cores of PM7 calculation. The red dash line is the ideal speed, which means if using 10 cores the speed will be increase 10 time with one core.

Figure 4.16 is the results from B3LYP and B3LYP-GD3 calculation, elapsed time of two methods are ploted. The results found that, for one core calculation B3LYP-GD3 gives the higher computational cost than B3LYP. So the previous results which express in the opposite way might be effected from the number of core. The different functionals is suitable with the different number of core, and 12 cores might increase the speed of GD3 correction.
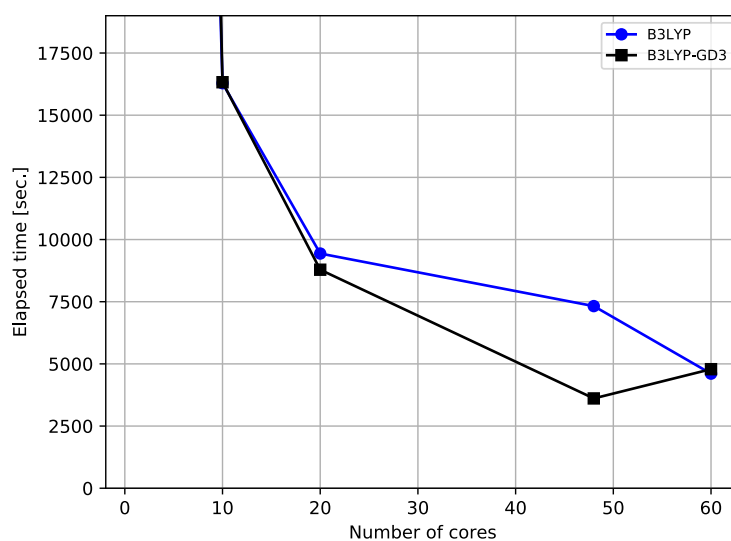
Figure 4.16: Elapsed time comparison between B3LYP and B3LYP-GD3 calculation. The result shows the after around ten cores DFT-GD3 spent less time in calculation than B3LYP.

For the formulation, the complexity of the B3LYP-GD3 is higher than B3LYP. Therefore, I expect that when the number of cores is increasing, B3LYP-GD3 can perform the calculation faster than B3LYP because the number of cores can serve in utilizing the complexity of B3LYP-GD3 in order to perform the vigorous computation. In the graph, B3LYP-GD3 and B3LYP perform similarly when the number of cores below 20. Nonetheless, when the number of cores is higher than 20, the computation time of B3LYP-GD3 decrease significantly comparing to B3LYP due to the effect of cores at this stage can support the higher complexity in B3LYP-GD3.

Table 4.7: The deviation of geometry optimization energy of inclusion complex (DEV$_{\text{comp}}$), hosts (DEV$_{\text{hosts}}$), and guest (DEV$_{\text{guest}}$) from average energies. The average energies of complexes (BCD, MBCD and HPBCD) are -3,089,919.95, -3,435,058.86 and -3,211,091.48. The average energies for the hosts are -2,682,323.08, -3,027,462.65 and -2,803,494.05 respectively. Finally, the average energy of plumbagin molecule is -407,576.43 (in kcal/mol).

functionals	DEV$_{\text{comp}}$	DEV$_{\text{hosts}}$	DEV$_{\text{guest}}$	E_{binding}	E_{raw}	$E_{\text{corrected}}$
CAMB3LYP	476.07	388.58	75.16	-8.13	-8.63	-3.80
	479.33			-4.86	-7.52	-2.11
	568.63	478.55		-4.86	-5.21	-1.27
	577.31			3.82	-7.03	-3.94
	503.33	411.78		-4.62	-6.06	-1.25
	502.10			-5.85	-6.61	-2.18
B3LYP-GD3	-939.07	-796.07	-134.09	-29.36	-32.49	-27.12
	-937.35			-27.64	-33.18	-27.37
	-1102.69	-951.15		-37.23	-30.63	-25.46
	-1090.66			-25.20	-30.93	-25.96
	-980.39	-838.42		-28.88	-33.38	-27.55
	-983.54			-32.04	-39.47	-33.23
M062X	400.07	350.47	49.21	-20.05	-23.78	-17.43
	398.75			-21.38	-26.05	-19.36
	460.66	417.93		-26.26	-23.05	-17.53
	470.99			-15.93	-17.29	-13.51
	417.90	368.95		-21.26	-28.53	-21.61
	418.36			-20.80	-25.49	-19.05
wB97XD	89.72	81.70	16.43	-28.84	-32.11	-26.59
	91.34			-27.22	-33.23	-27.24
	69.62	60.75		-27.34	-39.73	-22.19
	69.56			-27.40	-31.55	-26.63
	92.19	81.65		-26.88	-33.05	-26.99
	90.23			-28.85	-32.68	-26.88
M062X-GD3	379.88	338.45	48.67	-27.68	-31.49	-25.10
	378.37			-29.19	-33.87	-27.15
	433.45	399.44		-34.44	-29.97	-24.11
	439.52			-28.36	-33.52	-27.68
	396.10	355.86		-29.43	-36.87	-29.96
	396.65			-28.88	-34.77	-28.30
B3LYP	-745.23	-640.62	-122.51	-2.54	-3.40	1.02
	-746.25			-3.56	-4.27	0.65
	-876.80	-757.91		-16.16	-2.24	1.25
	-870.98			-10.33	-6.84	-4.86
	-784.02	-675.98		-6.52	-4.60	-0.87
	-777.42			0.07	-1.94	3.11
CAMB3LYP-GD3	336.14	277.51	67.16	-28.97	-31.83	-26.35
	338.19			-26.92	-32.48	-26.53
	411.91	352.41		-27.44	-29.89	-24.59
	439.52			0.17	-30.66	-25.58
	354.62	296.15		-29.68	-36.33	-30.42
	353.88			-30.43	-34.87	-29.16

Chapter 5

Summary

Docking technology is a promising solution for hard solubility and low physical/chemical stability of protein pharmaceuticals. However, it is difficult to artificially design good carriers because the pharmaceutical has to be released exactly near the target agent, for example. *Ab initio* calculation is expected to be a useful and powerful tool to elusidate the docking stability and the release process under different environments. However, their energitics cannot be described by *ab initio* calculations easily mainly due to significant contribution of dispersion forces.

We predicted docking stabilities between plumbagin and β-Cyclodextrins (β-Cyclodextrin, Methyl-β-Cyclodextrin, and Hydroxy Propyl-β-Cyclodextrin) by using density functional theory with different functionals in order to evaluate what functionals are able to give reliable answers. We used B3LYP and M06-2X functionals and their derivatives with DFT-GD3 and CAM corrections. In addition, we verified reliabilities of empirical methods, PM3, PM6, and PM7, which are usually used for proteins and large organic molecules today.

Although both B3LYP and M06-2X do not include dispersion force correction, only M06-2X reproduced stabilization by docking. The difference is likely to come from that different traing system sets are used to optimize their parameters: While those in B3LYP were optimized for just standard systems, M06-2X was trained even for systems where weak interactions contribute significantly to their formations. On the other hand, their DFT-GD3 correction derivatives, B3LYP-GD3 and M06-2X-GD3 functiontals, gave surprisingly similar predictions. GD3 corrections has been reported to significantly improve descrition of dispersion interactions by several works ever. Thus, the agreement is likely to be a consequence of that the functionals gave close values to the exact answer.

Our scope does not consider excited states and calculations of dynamic hyperpolarizabilities, so in this manner, CAM correction does not possess a distinct advantage. We still expect some small improvement over B3LYP, however, and this is reflected in the results for which CAM-B3LYP binding energy is slightly lower than B3LYP. Comparing to DFT-GD3 correction, it presents a significant correction to improve to near CCSD(T)-level results. We expect results for GD3 correction to be more precise and reliable. Calculation results are

largely in line with this expectation. GD3 correction manages to align disparate results from different XC functionals to a similar range of binding energies and trends, which shows the distinct advantage of GD3 over CAM in this matter.

Docking stabilities predicted by semi-empirical methods becomes larger in the order of PM3→PM6→PM7. First, for PM3→PM6, it is considered that newly added d-slater basis function slightly improved description of dispersion forces, in the same analogy of ($3pd$, $3df$) correction in Pople basis set. Second, the change of PM6→PM7 apparently comes from inclusion of the dispersion force correction. However, PM7 rather overestimated the values predicted by GD3 corrected functionals, which implies that semi-empirical approches are not reliable enough to design the carriers.
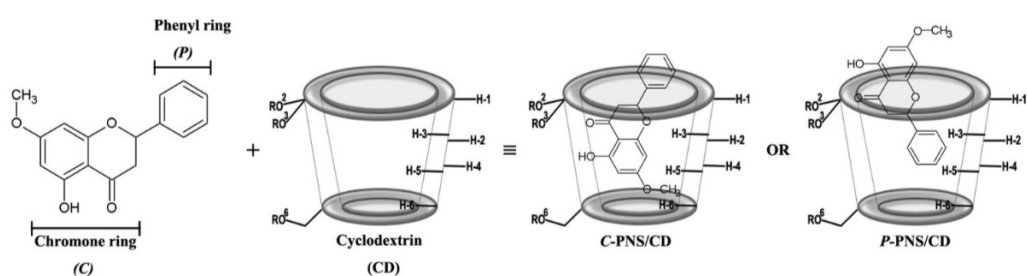
Figure 5.1: Similar system of host-guest interaction between guest (pinostrobin) and three hosts: BCD, 2,6-DMBCD and HPBCD, figure is taken from literature [10].

Further literature review, one study from Kicuntod *et al.* [10] is similar to our target system. Their experiment studied pinostrobin (PNS) as a host molecule encapsulated with three types of hosts. Three hosts include β-cyclodextrin (BCD), heptakis-(2,6-di-O-methyl)-β-cyclodextrin (2,6-DMBCD) and (2-hydroxypropyl)-β-cyclodextrin (HPBCD). They found the stability constants of all inclusion complexes at three different temperatures. Therefore, the stability constant is related to host-guest binding properties, and how strong of the interaction between two molecules. The graph between stability constant with the various temperatures used a Van't Hoff plot to find the thermodynamic property is presented in Table 5.1.

Table 5.1: Thermodynamics of three inclusion complexes derived from Van't Hoff plots [10].

Inclusion complex	ΔH (kcal/mol)	$T\Delta S$ (kcal/mol)	ΔG (kcal/mol)
PNS/BCD	-4.11	0.41	-4.49
PNS/2,6-DMBCD	0.23	5.47	-5.23
PNS/HPBCD	-3.61	1.29	-4.90

The negative binding energies of BCD and HPBCD suggest that the formation of inclusion complexes is an exothermic process. On the other hand, MBCD is a small positive (not

Table 5.2: Binding energy result of DFT-GD3 functionals, which consistent with the small difference observed between the binding energies of PNS/BCD and PNS/HPBCD in the work of Kicuntod or the experimental data.

Conformation	Experimental ΔH (kcal/mol)	B3LYP-GD3		CAM-B3LYP-GD3		M06-2X-GD3	
		Up	Down	Up	Down	Up	Down
HPBCD	-3.61	-27.55	-33.23	-30.42	-29.16	-29.96	-26.88
BCD	-4.11	-27.12	-27.37	-26.35	-26.53	-25.10	-27.24
MBCD	0.23	-25.46	-25.96	-24.59	-25.58	-24.10	-26.63

significant) endothermic process. The enthalpy results can be referred to the stability or the binding strength of the host-guest molecules. Their works provide order of stability as the following: PNS/BCD (-4.11 kcal/mol) > PNS/HPBCD (-3.61 kcal/mol) >PNS/2,6-DMBCD (0.23 kcal/mol). This trend is largely reflected in our results with GD3 functionals, which in general follows the stability trend HPBCD > BCD > MBCD. It is consistent with the small difference observed between the binding energies of PNS/BCD and PNS/HPBCD in the work of Kicuntod *et al.*, for which a reversal of order in 0 K is not unlikely.

Another similar case is from Lukin *et al.*, their work calculated the 6-[4-[N-tert- Butoxy-carbonyl N-(N'-ethyl)propanamide]imidazolyl]-6-deoxycyclomaltoheptaose encapsulation complex of with BCD by using B3LYP-GD3 and the binding energies are -41.3 to -33.4 kcal/mol. The result of our system is between -27.37 to -27.12 kcal/mol. Our guest molecule is smaller size and has the different chemical group. The larger size of host may cause the steric force and increase binding energy between these two molecules. In addition, their guest molecule consist N and S, which our guest molecule does not. Especially, N atom can increase the possibility to form H-bond with host, which can cause the higher binding energy result.

In general, the findings of this research are valid for the inter-molecular system. The host-guest interaction of our target system is the interaction between two organic molecules, in which the dipole-dipole interaction plays an the important role in this inter-molecular interaction. The results are also applicable to other systems dominated by inter-molecular bindings, dispersion force, van der Waals or long-range interaction. These systems generally possess relatively small stabilization energy of 1-20 kcal/mol (as compared to covalent bond stabilization energy of around 100 kcal/mol).

For inter-molecular interactions, a general pattern has been observed, generally independent of the interacting molecules. A $1/R^6$ behaviour is prominent for these long-range interactions. This is reflected within DFT-GD3 correction, which makes use of this fact as an empirical term. This general pattern means that other systems for which dispersion forces are dominant can make use of the results presented in this work.

Appendix A

Conversion Units

Appendix A provide the conversion factors for energy units in Table A.1. The units have been used throughout this thesis,

Table A.1: Conversion factors for energy units.

	Hartree	eV	cm^{-1}	kcal/mol	kJ/mol
Hartree	1	27.2116	219474.63	627.509	2625.5
eV	0.0367493	1	8065.73	23.0609	96.4869
cm^{-1}	4.55633×10^{-6}	1.23981×10^{-4}	1	0.00285911	0.0119627
kcal/mol	0.00159360	0.0433634	349.759	1	4.18400
kJ/mol	0.00038088	0.01036410	83.593	0.239001	1

References

[1] A. Burodom and A. Itharat, "Inflammatory suppressive effect of benjakul , a thai traditional medicine on intestinal epithelial cell line," *Journal of Medicinal Plants Research*, vol. 7, no. 44, pp. 3286–3291, 2013.

[2] M. Suthanurak, I. Sakpakdeejaroen, R. Rattarom, and A. Itharat, "Formulation and stability test of bj adaptogen tablets for cancer treatment," *Planta Medica*, vol. 76, no. 12, pp. 160–163, 2010.

[3] G. Astray, C. Gonzalez-Barreiro, J. C. Mejuto, R. Rial-Otero, and J. Simal-Gandara, "A review on the use of cyclodextrins in foods," *Food Hydrocoll.*, vol. 23, no. 7, pp. 1631–1640, 2009.

[4] P. Sompornpisut, N. Deechalao, and J. Vongsvivut, "An inclusion complex of β-cyclodextrin-lphenylalanine: 1h nmr and molecular docking studies," *ScienceAsia*, vol. 28, no. 3, p. 263, 2002. [Online]. Available: http://www.scienceasia.org/2002.28.n3/263.php

[5] A. Martinez-Alonso, S. Losada-Barreiro, and C. Bravo-Diaz, "Encapsulation and solubilization of the antioxidants gallic acid and ethyl, propyl and butyl gallate with β-cyclodextrin," *J. Mol. Liq.*, vol. 210, pp. 143–150, 2015. [Online]. Available: http://dx.doi.org/10.1016/j.molliq.2014.12.016

[6] E. M. M. Del Valle, "Cyclodextrins and their uses: A review," *Process Biochemistry*, vol. 39, no. 9, pp. 1033–1046, 2004.

[7] H. Dodziuk, *Cyclodextrins and Their Complexes*. Weinheim, FRG: Wiley-VCH Verlag GmbH and Co. KGaA, May 2006. [Online]. Available: http://doi.wiley.com/10.1002/3527608982

[8] K. S. C., "Gaussian basis sets." [Online]. Available: https://www.southampton.ac.uk/assets/centresresearch/documents/compchem/DFT{_}L8.pdf

[9] S. Grimme, "Density functional theory with london dispersion corrections," *Wiley Interdiscip. Rev. Comput. Mol. Sci.*, vol. 1, no. 2, pp. 211–228, mar 2011. [Online]. Available: http://doi.wiley.com/10.1002/wcms.30

[10] J. Kicuntod, K. Sangpheak, M. Mueller, P. Wolschann, H. Viernstein, S. Yanaka, K. Kato, W. Chavasiri, P. Pongsawasdi, N. Kungwan, and T. Rungrotmongkol, "Theoretical and experimental studies on inclusion complexes of pinostrobin and beta-cyclodextrins," *Scientia Pharmaceutica*, vol. 86, no. 1, 2018. [Online]. Available: http://www.mdpi.com/2218-0532/86/1/5

[11] "Cyclodextrin containing products." [Online]. Available: https://notendur.hi.is/thorstlo/cyclodextrin.pdf

[12] Aree, Hoier, Schulz, Reck, and Saenger, "Novel type of thermostable channel clathrate hydrate formed by heptakis(2,6-di-o-methyl)-beta-cyclodextrin small middle dot15 h(2)o-a paradigm of the hydrophobic effect topography of cyclodextrin inclusion complexes," *Angewandte Chemie (International ed. in English)*, vol. 39, no. 5, pp. 897–899, mar 2000. [Online]. Available: http://www.ncbi.nlm.nih.gov/pubmed/10760885

[13] R. Sure and S. Grimme, "Comprehensive Benchmark of Association (Free) Energies of Realistic Host-Guest Complexes," *Journal of Chemical Theory and Computation*, vol. 11, no. 8, pp. 3785–3801, 2015.

[14] K. Hongo and R. Maezono, "A Computational Scheme To Evaluate Hamaker Constants of Molecules with Practical Size and Anisotropy," *Journal of Chemical Theory and Computation*, vol. 13, no. 11, pp. 5217–5230, nov 2017. [Online]. Available: http://pubs.acs.org/doi/10.1021/acs.jctc.6b01159

[15] M. J. Frisch, G. W. Trucks, H. B. Schlegel, G. E. Scuseria, M. A. Robb, J. R. Cheeseman, G. Scalmani, V. Barone, B. Mennucci, G. A. Petersson, H. Nakatsuji, M. Caricato, X. Li, H. P. Hratchian, A. F. Izmaylov, J. Bloino, G. Zheng, J. L. Sonnenberg, M. Hada, M. Ehara, K. Toyota, R. Fukuda, J. Hasegawa, M. Ishida, T. Nakajima, Y. Honda, O. Kitao, H. Nakai, T. Vreven, J. A. Montgomery, Jr., J. E. Peralta, F. Ogliaro, M. Bearpark, J. J. Heyd, E. Brothers, K. N. Kudin, V. N. Staroverov, R. Kobayashi, J. Normand, K. Raghavachari, A. Rendell, J. C. Burant, S. S. Iyengar, J. Tomasi, M. Cossi, N. Rega, J. M. Millam, M. Klene, J. E. Knox, J. B. Cross, V. Bakken, C. Adamo, J. Jaramillo, R. Gomperts, R. E. Stratmann, O. Yazyev, A. J. Austin, R. Cammi, C. Pomelli, J. W. Ochterski, R. L. Martin, K. Morokuma, V. G. Zakrzewski, G. A. Voth, P. Salvador, J. J. Dannenberg, S. Dapprich, A. D. Daniels, Ã. Farkas, J. B. Foresman, J. V. Ortiz, J. Cioslowski, and D. J. Fox, "Gaussian09 revision e.01," gaussian Inc. Wallingford CT 2009.

[16] R. Dennington, T. Keith, and J. Millam, "Gaussview version 5," semichem Inc. Shawnee Mission KS 2009.

[17] O. Srihakulung, L. Lawtrakul, P. Toochinda, W. Kongprawechnon, A. Intarapanich, and R. Maezono, "Theoretical investigation of molecular calculations on inclusion complexes of plumbagin with β-cyclodextrins," in *2017 Fourth Asian Conf. Def. Technol. - Japan.* IEEE, nov 2017, pp. 1–5. [Online]. Available: http://ieeexplore.ieee.org/document/8259589/

[18] R. Rattarom, I. Sakpakdeejaroen, and A. Itharat, "Cytotoxic effects of the ethanolic extract from benjakul formula and its compounds on human lung cancer cells," *Thai Journal of Pharmacology*, vol. 32, no. 1, pp. 99–101, 2010.

[19] Saetung, Athima, Itharat, Arunporn, Dechsukum, Chawaboon, Wattanapiromsakul, Chatchai, N. K. Keaw, and P. Ratanasuwan, "Cytotoxic activity of thai medicinal plants for cancer treatment," *J Sci Technol*, vol. 27, no. Suppl. 2, pp. 469–478, 2005. [Online]. Available: http://www.aseanbiodiversity.info/Abstract/53004077.pdf

[20] L. van der Vijver, "Distribution of plumbagin in the mplumbaginaceae," *Phytochemistry*, vol. 11, no. 11, pp. 3247–3248, nov 1972. [Online]. Available: http://linkinghub.elsevier.com/retrieve/pii/S0031942200863803

[21] H. Rischer, A. Hamm, and G. Bringmann, "Nepenthes insignis uses a c2-portion of the carbon skeleton of l-alanine acquired via its carnivorous organs, to build up the allelochemical plumbagin," *Phytochemistry*, vol. 59, no. 6, pp. 603–609, mar 2002. [Online]. Available: http://linkinghub.elsevier.com/retrieve/pii/S0031942202000031

[22] T. G. Son, S. Camandola, T. V. Arumugam, R. G. Cutler, R. S. Telljohann, M. R. Mughal, T. A. Moore, W. Luo, Q.-S. Yu, D. A. Johnson, J. A. Johnson, N. H. Greig, and M. P. Mattson, "Plumbagin, a novel nrf2/are activator, protects against cerebral ischemia," *Journal of Neurochemistry*, vol. 112, no. 5, pp. 1316–1326, mar 2010. [Online]. Available: http://doi.wiley.com/10.1111/j.1471-4159.2009.06552.x

[23] S. Sugie, K. Okamoto, K. M. Rahman, T. Tanaka, K. Kawai, J. Yamahara, and H. Mori, "Inhibitory effects of plumbagin and juglone on azoxymethane-induced intestinal carcinogenesis in rats." *Cancer letters*, vol. 127, no. 1-2, pp. 177–83, may 1998. [Online]. Available: http://www.ncbi.nlm.nih.gov/pubmed/9619875

[24] Y.-L. Hsu, "Plumbagin (5-hydroxy-2-methyl-1,4-naphthoquinone) induces apoptosis and cell cycle arrest in a549 cells through p53 accumulation via c-jun nh2-terminal kinase-mediated phosphorylation at serine 15 in vitro and in vivo," *Journal of Pharmacology and Experimental Therapeutics*, vol. 318, no. 2, pp. 484–494, mar 2006. [Online]. Available: http://jpet.aspetjournals.org/cgi/doi/10.1124/jpet.105.098863

[25] S. J. Risch, *Encapsulation: Overview of Uses and Techniques.* ACS Publications, 1995, ch. 1, pp. 2–7. [Online]. Available: https://pubs.acs.org/doi/abs/10.1021/bk-1995-0590.ch001

[26] A. Rasheed, A. Kumar C.K., and V. V. N. S. S. Sravanthi, "Cyclodextrins as drug carrier molecule: A review," *Scientia Pharmaceutica*, vol. 76, no. 4, pp. 567–598, 2008.

[27] A. C. Villiers, "Sur la transformation de la feìcule en dextrine par le ferment butyrique," *Seances Acad. Sci.*, vol. 112, no. 536538, 1891.

[28] T. Loftsson and D. Duchene, "Cyclodextrins and their pharmaceutical applications," *International Journal of Pharmaceutics*, vol. 329, no. 1-2, pp. 1–11, 2007.

[29] C. R. Dass and W. Jessup, "Apolipoprotein a-i, cyclodextrins and liposomes as potential drugs for the reversal of atherosclerosis. a review." *The Journal of pharmacy and pharmacology*, vol. 52, no. 7, pp. 731–761, 2000.

[30] M. Singh, R. Sharma, and U. C. Banerjee, "Biotechnological applications of cyclodextrins." *Biotechnology advances*, vol. 20, no. 5-6, pp. 341–59, dec 2002. [Online]. Available: http://www.ncbi.nlm.nih.gov/pubmed/14550020

[31] J. Szejtli, "Introduction and general overview of cyclodextrin chemistry," *Chemical Reviews*, vol. 98, no. 5, pp. 1743–1754, jul 1998. [Online]. Available: http://pubs.acs.org/doi/abs/10.1021/cr970022c

[32] R. A. Rajewski and V. J. Stella, "Pharmaceutical applications of cyclodextrins. 2. in vivo drug delivery," *Journal of Pharmaceutical Sciences*, vol. 85, no. 11, pp. 1142–1169, 1996.

[33] P. Dandawate, K. Vemuri, K. Venkateswara Swamy, E. M. Khan, M. Sritharan, and S. Padhye, "Synthesis, characterization, molecular docking and anti-tubercular activity of plumbagin-isoniazid analog and its β-cyclodextrin conjugate," *Bioorganic and Medicinal Chemistry Letters*, vol. 24, no. 21, pp. 5070–5075, 2014. [Online]. Available: http://dx.doi.org/10.1016/j.bmcl.2014.09.032

[34] U. V. Singh and N. Udupa, "Reduced toxicity and enhanced antitumor efficacy of betacyclodextrin plumbagin inclusion complex in mice bearing ehrlich ascites carcinoma," *Indian Journal of Physiology and Pharmacology*, vol. 41, no. 2, pp. 171–175, 1997.

[35] A. Magnusdottir, M. Masson, and T. Loftsson, "Self association and cyclodextrin solubilization of nsaids," in *J. Incl. Phenom.*, vol. 44, 2002, pp. 213–218.

[36] L. Lawtrakul, K. Inthajak, and P. Toochinda, "Molecular calculations on β-cyclodextrin inclusion complexes with five essential oil compounds from Ocimum basilicum (sweet basil)," *ScienceAsia*, vol. 40, no. 2, pp. 145–151, 2014.

[37] N. Leila, H. Sakina, A. Bouhadiba, M. Fatiha, and L. Leila, "Molecular modeling investigation of para-nitrobenzoic acid interaction in β-cyclodextrin," *Journal of Molecular Liquids*, vol. 160, no. 1, pp. 1–7, 2011. [Online]. Available: http://dx.doi.org/10.1016/j.molliq.2011.02.004

[38] S. Seridi, A. Seridi, M. Berredjem, and M. Kadri, "Host-guest interaction between 3,4-dihydroisoquinoline-2(1H)-sulfonamide and β-cyclodextrin: Spectroscopic and molecular modeling studies," *J. Mol. Struct.*, vol. 1052, pp. 8–16, 2013. [Online]. Available: http://dx.doi.org/10.1016/j.molstruc.2013.08.035

[39] L. Abdelmalek, M. Fatiha, N. Leila, C. Mouna, M. Nora, and K. Djameleddine, "Computational study of inclusion complex formation between carvacrol and β-cyclodextrin in vacuum and in water: Charge transfer, electronic transitions and NBO analysis," *J. Mol. Liq.*, vol. 224, pp. 62–71, 2016. [Online]. Available: http://dx.doi.org/10.1016/j.molliq.2016.09.053

[40] A. Bouhadiba, Y. Belhocine, M. Rahim, I. Djilani, L. Nouar, and D. E. Khatmi, "Host-guest interaction between tyrosine and β-cyclodextrin: Molecular modeling and nuclear studies," *J. Mol. Liq.*, vol. 233, pp. 358–363, 2017. [Online]. Available: http://www.sciencedirect.com/science/article/pii/S0167732216338582

[41] I. Djilani, L. Nouar, F. Madi, S. Haiahem, A. Bouhadiba, and D. Khatmi, *Molecular modeling study of neutral and cationic species of ortho-anisidine by β-cyclodextrin*. Elsevier Inc., 2014, vol. 68. [Online]. Available: http://dx.doi.org/10.1016/B978-0-12-800536-1.00015-0

[42] E. H. Santos, J. A. Kamimura, L. E. Hill, and C. L. Gomes, "Characterization of carvacrol beta-cyclodextrin inclusion complexes as delivery systems for antibacterial and antioxidant applications," *LWT - Food Sci. Technol.*, vol. 60, no. 1, pp. 583–592, 2015. [Online]. Available: http://dx.doi.org/10.1016/j.lwt.2014.08.046

[43] L. E. Hill, C. Gomes, and T. M. Taylor, "Characterization of beta-cyclodextrin inclusion complexes containing essential oils (trans-cinnamaldehyde, eugenol, cinnamon bark, and clove bud extracts) for antimicrobial delivery applications," *LWT - Food Sci. Technol.*, vol. 51, no. 1, pp. 86–93, 2013. [Online]. Available: http://dx.doi.org/10.1016/j.lwt.2012.11.011

[44] W. Saenger and T. Steiner, "Cyclodextrin inclusion complexes: Host-guest interactions and hydrogen-bonding networks," *Acta Crystallogr. Sect. A Found. Crystallogr.*, vol. 54, no. 6, pp. 798–805, 1998.

[45] A. H. Asterten Kjell; Meland, Inge, "Activities and phase diagram data of nafalf3al2o3 mixtures derived from electromotive force and cryoscopic measurements. standard thermodynamic data of beta-al2o3(s), na3alf6(s), na5al3f14(s) and naalf4(l)," *Acta Chem. Scand.*, vol. 36 A, pp. 323–327, 1982. [Online]. Available: http://actachemscand.org/doi/10.3891/acta.chem.scand.36a-0323

[46] M. Sakurai, M. Kitagawa, H. Hoshi1, Y. Inoue, and R. Chujo, "A molecular orbital study of cyclodextrin (cyclomalto-oligosaccharide) inclusion complexes. iii, dipole moments of cyclodextrins in various types of inclusion complex," *Carbohydr. Res.*, vol. 198, pp. 181–191, 1990.

[47] A. Rafati, S. Hashemianzadeh, Z. Nojini, and M. Safarpour, "Theoretical study of the inclusion complexes of α and β-cyclodextrins with decyltrimethylammonium bromide (dtab) and tetradecyltrimethylammonium bromide (ttab)," *Journal of Molecular Liquids*, vol. 135, no. 1-3, pp. 153–157, jul 2007.

[48] H. Messiad, T. Yousfi, R. Djemil, and H. Amira-Guebailia, "Modeling of the inclusive complexation of natural drug trans 3,5,3,4-tetrahydroxystilbene with β-cyclodextrin," *Comptes Rendus Chimie*, pp. 1–10, 2016. [Online]. Available: http://linkinghub.elsevier.com/retrieve/pii/S1631074816302351

[49] T. Walter, *Perspectives on Semiempirical Molecular Orbital Theory*. Wiley-Blackwell, 2007, pp. 703–757. [Online]. Available: https://onlinelibrary.wiley.com/doi/abs/10.1002/9780470141526.ch10

[50] T. Aree, R. Arunchai, N. Koonrugsa, and A. Intasiri, "Fluorometric and theoretical studies on inclusion complexes of β-cyclodextrin and d-, l-phenylalanine," *Spectrochim. Acta - Part A Mol. Biomol. Spectrosc.*, vol. 96, pp. 736–743, 2012. [Online]. Available: http://dx.doi.org/10.1016/j.saa.2012.07.049

[51] L. Xiao-Song, L. Lei, M. Ting-Wei, and G. Qing-Xiang, "A systematic quantum chemistry study on cyclodextrins," *Monatshefte fuer Chemie/Chemical Mon.*, vol. 131, no. 8, pp. 849–855, 2000. [Online]. Available: http://www.springerlink.com/index/10.1007/s007060070062

[52] W. J. Hehre, *A Guide to Molecular Mechanics and Quantum Chemical Calculations*. Wavefunction, 2003. [Online]. Available: https://www.wavefun.com/support/AGuidetoMM.pdf

[53] A. Antony Muthu Prabhu, V. K. Subramanian, and N. Rajendiran, "Excimer formation in inclusion complexes of β-cyclodextrin with salbutamol, sotalol and atenolol: Spectral and molecular modeling studies," *Spectrochim. Acta - Part A Mol. Biomol. Spectrosc.*, vol. 96, pp. 95–107, 2012. [Online]. Available: http://dx.doi.org/10.1016/j.saa.2012.04.044

[54] J. J. P. Stewart, "Optimization of parameters for semiempirical methods V: Modification of NDDO approximations and application to 70 elements," *J. Mol. Model.*, vol. 13, no. 12, pp. 1173–1213, oct 2007. [Online]. Available: http://link.springer.com/10.1007/s00894-007-0233-4

[55] A. A. Voityuk and N. Rosch, "Am1/d parameters for molybdenum," *J. Phys. Chem. A*, vol. 104, no. 17, pp. 4089–4094, 2000.

[56] M. Rahim, F. Madi, L. Nouar, A. Bouhadiba, S. Haiahem, D. E. Khatmi, and Y. Belhocine, "Driving forces and electronic structure in β-cyclodextrin/3,3-diaminodiphenylsulphone complex," *J. Mol. Liq.*, vol. 199, pp. 501–510, 2014. [Online]. Available: http://dx.doi.org/10.1016/j.molliq.2014.09.035

[57] Y. Xia, X. Wang, Y. Zhang, and B. Luo, "Theoretical Study on Interactions of β-cyclodextrin with Trans-dichloro(dipyridine) platinum(II)," *Comput. Theor. Chem.*, vol. 967, no. 2-3, pp. 213–218, 2011. [Online]. Available: http://dx.doi.org/10.1016/j.comptc.2011.03.010

[58] F. O. Suliman and A. A. Elbashir, "Enantiodifferentiation of chiral baclofen by β-cyclodextrin using capillary electrophoresis: A molecular modeling approach," *J. Mol. Struct.*, vol. 1019, pp. 43–49, 2012. [Online]. Available: http://dx.doi.org/10.1016/j.molstruc.2012.03.055

[59] E. E. Eid, A. B. Abdul, F. E. O. Suliman, M. A. Sukari, A. Rasedee, and S. S. Fatah, "Characterization of the inclusion complex of zerumbone with hydroxypropyl-β-cyclodextrin," *Carbohydr. Polym.*, vol. 83, no. 4, pp. 1707–1714, 2011. [Online]. Available: http://dx.doi.org/10.1016/j.carbpol.2010.10.033

[60] M. I. Sancho, E. Gasull, S. E. Blanco, and E. A. Castro, "Inclusion complex of 2-chlorobenzophenone with cyclomaltoheptaose (β-cyclodextrin): Temperature, solvent effects and molecular modeling," *Carbohydr. Res.*, vol. 346, no. 13, pp. 1978–1984, 2011. [Online]. Available: http://dx.doi.org/10.1016/j.carres.2011.05.002

[61] J. J. Stewart, "Optimization of parameters for semiempirical methods VI: More modifications to the NDDO approximations and re-optimization of parameters," *J. Mol. Model.*, vol. 19, no. 1, pp. 1–32, 2013.

[62] A. D. Bani-Yaseen, "Computational molecular perspectives on the interaction of propranolol with β-cyclodextrin in solution: Towards the drug-receptor mechanism of interaction," *Journal of Molecular Liquids*, 2016. [Online]. Available: http://linkinghub.elsevier.com/retrieve/pii/S0167732216331397

[63] A. Bouzitouna, D. Khatmi, and O. Attoui-Yahia, "A hybrid mp2/dft scheme for n-nitroso-n-(2-chloroethyl)-n'-sulfamoylprolinate/β-cyclodextrin supramolecular structure: Aim, nbo analysis," *Computational and Theoretical Chemistry*, 2016. [Online]. Available: http://www.sciencedirect.com/science/article/pii/S2210271X1630490X

[64] A. S. Archimandritis, T. Papadimitriou, K. A. Kormas, C. S. Laspidou, K. Yannakopoulou, and Y. G. Lazarou, "Theoretical investigation of microcystin-LR, microcystin-RR and nodularin-R complexation with α-, β-, and γ-cyclodextrin as a starting point for the targeted design of efficient cyanotoxin traps," *Sustain. Chem. Pharm.*, vol. 3, pp. 25–32, 2016. [Online]. Available: http://dx.doi.org/10.1016/j.scp.2016.02.001

[65] X. Barrila and R. Solivab, *Molecular Modelling*. Royal Society of Chemistry, 2006, vol. 2. [Online]. Available: papers://7ed92360-9572-4d78-9cbf-e00535d02a25/Paper/p51

[66] Y. Zhao, N. E. Schultz, and D. G. Truhlar, "Design of density functionals by combining the method of constraint satisfaction with parametrization for thermochemistry, thermochemical kinetics, and noncovalent interactions," *Journal of Chemical Theory and Computation*, vol. 2, no. 2, pp. 364–382, 2006.

[67] T. Y. Zhao and D. G., "Comparative DFT study of van der Waals complexes: Rare-gas dimers, alkaline-earth dimers, zinc dimer and zinc-rare-gas dimers," *Journal of Physical Chemistry A*, vol. 110, no. 15, pp. 5121–5129, 2006.

[68] Y. Zhao and D. G. Truhlar, "Hybrid meta density functional theory methods for thermochemistry, thermochemical kinetics, and noncovalent interactions: The MPW1B95 and MPWB1K models and comparative assessments for hydrogen bonding and van der Waals interactions," *Journal of Physical Chemistry A*, vol. 108, no. 33, pp. 6908–6918, 2004.

[69] T. Zhao, Yan and D. G., "The M06 suite of density functionals for main group thermochemistry, thermochemical kinetics, noncovalent interactions, excited states, and transition elements: Two new functionals and systematic testing of four M06-class functionals and 12 other functionals," *Theor. Chem. Acc.*, vol. 120, no. 1-3, pp. 215–241, 2008.

[70] O. A. Von Lilienfeld, I. Tavernelli, U. Rothlisberger, and D. Sebastiani, "Variational optimization of effective atom centered potentials for molecular properties," *Journal of Chemical Physics*, vol. 122, no. 1, pp. 1–7, 2005.

[71] J.-D. Chai and M. Head-Gordon, "Long-range corrected hybrid density functionals with damped atom–atom dispersion corrections," *Phys. Chem. Chem. Phys.*, vol. 10, no. 44, p. 6615, 2008. [Online]. Available: http://xlink.rsc.org/DOI=b810189b

[72] S. Grimme, J. Antony, S. Ehrlich, and H. Krieg, "A consistent and accurate ab initio parametrization of density functional dispersion correction (DFT-D) for the 94 elements H-Pu," *J. Chem. Phys.*, vol. 132, no. 15, 2010.

[73] A. Gulans, M. J. Puska, and R. M. Nieminen, "Linear-scaling self-consistent implementation of the van der Waals density functional," *Physical Review B - Condensed Matter and Materials Physics*, vol. 79, no. 20, 2009.

[74] T. Yanai, D. P. Tew, and N. C. Handy, "A new hybrid exchange-correlation functional using the Coulomb-attenuating method (CAM-B3LYP)," *Chem. Phys. Lett.*, vol. 393, no. 1-3, pp. 51–57, 2004.

[75] K. Okuno, Y. Shigeta, R. Kishi, H. Miyasaka, and M. Nakano, "Tuned CAM-B3LYP functional in the time-dependent density functional theory scheme for excitation energies and properties of diarylethene derivatives," *Journal of Photochemistry and Photobiology A: Chemistry*, 2012.

[76] P. A. Limacher, K. V. Mikkelsen, and H. P. Lüthi, "On the accurate calculation of polarizabilities and second hyperpolarizabilities of polyacetylene oligomer chains using the CAM-B3LYP density functional," *Journal of Chemical Physics*, vol. 130, no. 19, 2009.

[77] M. Soniat, D. M. Rogers, and S. B. Rempe, "Dispersion- and Exchange-Corrected Density Functional Theory for Sodium Ion Hydration," *Journal of Chemical Theory and Computation*, vol. 11, no. 7, pp. 2958–2967, 2015.

[78] B. Brauer, M. K. Kesharwani, and J. M. Martin, "Some observations on counterpoise corrections for explicitly correlated calculations on noncovalent interactions," *Journal of Chemical Theory and Computation*, vol. 10, no. 9, pp. 3791–3799, 2014.

[79] J. Witte, N. Mardirossian, J. B. Neaton, and M. Head-Gordon, "Assessing DFT-D3 Damping Functions Across Widely Used Density Functionals: Can We Do Better?" *Journal of Chemical Theory and Computation*, vol. 13, no. 5, pp. 2043–2052, 2017.

[80] J. F. Dobson, A. White, and A. Rubio, "Asymptotics of the dispersion interaction: Analytic benchmarks for van der Waals energy functionals," *Physical Review Letters*, 2006.

[81] J. Chen and K. N. Houk, "Molecular Modeling: Principles and Applications By Andrew R. Leach. Addison Wesley Longman Limited: Essex, England, 1996. 595 pp. ISBN 0-582-23933-8. $35," *J. Chem. Inf. Comput. Sci.*, vol. 38, no. 5, pp. 939–939, sep 1998. [Online]. Available: http://pubs.acs.org/doi/abs/10.1021/ci9804241

[82] N. L. Chekirou, I. Benomrane, F. Lebsir, and A. M. Krallafa, "Theoretical and experimental study of the tetracain/β-cyclodextrin inclusion complex," *Journal of Inclusion Phenomena and Macrocyclic Chemistry*, vol. 74, no. 1-4, pp. 211–221, 2012.

[83] M. J. Jenita, G. Venkatesh, V. K. Subramanian, and N. Rajendiran, "Twisted intramolecular charge transfer effects on fast violet b and fast blue rr: Effect of hp-α- and hp-β-cyclodextrins," *Journal of Molecular Liquids*, vol. 178, pp. 160–167, 2013. [Online]. Available: http://dx.doi.org/10.1016/j.molliq.2012.11.033

[84] K. Paramasivaganesh, K. Srinivasan, A. Manivel, S. Anandan, K. Sivakumar, S. Radhakrishnan, and T. Stalin, "Studies on inclusion complexation between 4,4-dihydroxybiphenyl and β-cyclodextrin by experimental and theoretical approach," *Journal of Molecular Structure*, vol. 1048, pp. 399–409, 2013. [Online]. Available: http://dx.doi.org/10.1016/j.molstruc.2013.04.072

[85] S. Haiahem, L. Nouar, I. Djilani, A. Bouhadiba, F. Madi, and D. E. Khatmi, "Host-guest inclusion complex between -cyclodextrin and paeonol: A theoretical approach," *Comptes Rendus Chimie*, vol. 16, no. 4, pp. 372–379, 2013. [Online]. Available: http://dx.doi.org/10.1016/j.crci.2012.11.008

[86] S. Sapte and Y. Pore, "Inclusion complexes of cefuroxime axetil with β-cyclodextrin: Physicochemical characterization, molecular modeling and effect of l-arginine on complexation," *Journal of Pharmaceutical Analysis*, vol. 6, no. 5, pp. 300–306, 2016. [Online]. Available: http://www.sciencedirect.com/science/article/pii/S2095177916300120

[87] X. Zhu, G. Wu, and D. Chen, "Molecular dynamics simulation of cyclodextrin aggregation and extraction of anthracene from non-aqueous liquid phase," *Journal of Hazardous Materials*, vol. 320, pp. 169–175, 2016. [Online]. Available: http://linkinghub.elsevier.com/retrieve/pii/S0304389416307361

[88] A. Zaboub, F. Madi, R. Merdes, M. Mohamedi, and L. Nouar, "A combined dft and experimental study of proline/β-cyclodextrin inclusion complex," *Journal*

of Molecular Liquids, vol. 216, pp. 716–723, 2016. [Online]. Available: http://dx.doi.org/10.1016/j.molliq.2016.01.082

[89] H. Cao, M. Wang, K. Nie, X. Zhang, M. Lei, L. Deng, F. Wang, and T. Tan, "β-cyclodextrin as an additive to improve the thermostability of yarrowia lipolytica lipase 2: Experimental and simulation insights," *Journal of the Taiwan Institute of Chemical Engineers*, vol. 0, pp. 1–7, 2016. [Online]. Available: http://linkinghub.elsevier.com/retrieve/pii/S1876107016304254

[90] A. Farcas, A. Fifere, I. Stoica, F. Farcas, and A. M. Resmerita, "Thermal analysis and theoretical study of Alpha-cyclodextrin azomethine [2]-rotaxane formation by semi-empirical method PM3," *Chem. Phys. Lett.*, vol. 514, no. 1-3, pp. 74–78, 2011. [Online]. Available: http://dx.doi.org/10.1016/j.cplett.2011.08.007

[91] D. Kubota, O. F. L. MacEdo, G. R. S. Andrade, L. S. Conegero, L. E. Almeida, N. B. Costa, and I. F. Gimenez, "Structural and theoretical-experimental physicochemical study of trimethoprim/randomly methylated-beta-cyclodextrin binary system," *Carbohydr. Res.*, vol. 346, no. 17, pp. 2746–2751, 2011. [Online]. Available: http://dx.doi.org/10.1016/j.carres.2011.09.030

[92] Y. Liao, X. Zhang, C. Li, Y. Huang, M. Lei, M. Yan, Y. Zhou, and C. Zhao, "Inclusion complexes of HP-Beta-cyclodextrin with agomelatine: Preparation, characterization, mechanism study and in vivo evaluation," *Carbohydr. Polym.*, vol. 147, pp. 415–425, 2016. [Online]. Available: http://dx.doi.org/10.1016/j.carbpol.2016.04.022

[93] N. Bensouilah and M. Abdaoui, "Inclusion complex of n-nitroso, n-(2-chloroethyl), n', n'-dibenzylsulfamid with β-cyclodextrin: Fluorescence and molecular modeling," *Comptes Rendus Chim.*, vol. 15, no. 11-12, pp. 1022–1036, 2012. [Online]. Available: http://dx.doi.org/10.1016/j.crci.2012.09.004

[94] S. Chaudhuri, S. Chakraborty, and P. K. Sengupta, "Encapsulation of serotonin in Beta-cyclodextrin nano-cavities: Fluorescence spectroscopic and molecular modeling studies," *J. Mol. Struct.*, vol. 975, no. 1-3, pp. 160–165, 2010. [Online]. Available: http://dx.doi.org/10.1016/j.molstruc.2010.04.014

[95] Y. Izadmanesh and J. B. Ghasemi, "Thermodynamic study of β-cyclodextrin-dye inclusion complexes using gradient flow injection technique and molecular modeling," *Spectrochim. Acta Part A Mol. Biomol. Spectrosc.*, vol. 165, pp. 54–60, 2016. [Online]. Available: http://www.sciencedirect.com/science/article/pii/S1386142516302086

[96] D. Prema and K. Sivakumar, "Inclusion complexation of acetanilide into the β-cyclodextrin nanocavity: A computational approach," *Procedia Mater.*

Sci., vol. 10, no. Cnt 2014, pp. 467–475, 2015. [Online]. Available: http://linkinghub.elsevier.com/retrieve/pii/S2211812815003211

[97] L. Seridi and A. Boufelfel, "Molecular modeling study of Lamotrigine/beta-cyclodextrin inclusion complex," *J. Mol. Liq.*, vol. 158, no. 2, pp. 151–158, 2011. [Online]. Available: http://dx.doi.org/10.1016/j.molliq.2010.11.011

[98] C. M. Fernandes, R. A. Carvalho, S. Pereira da Costa, and F. J. B. Veiga, "Multimodal molecular encapsulation of nicardipine hydrochloride by β-cyclodextrin, hydroxypropyl-β-cyclodextrin and triacetyl-β-cyclodextrin in solution. Structural studies by 1H NMR and ROESY experiments," *Eur. J. Pharm. Sci.*, vol. 18, no. 5, pp. 285–296, 2003.

[99] G. M. Morris, D. S. Goodsell, R. S. Halliday, R. Huey, W. E. Hart, R. K. Belew, and A. J. Olson, "Automated docking using a lamarckian genetic algorithm and an empirical binding free energy function," *J. Comput. Chem.*, vol. 19, no. 14, pp. 1639–166, nov 1998.

[100] D. S. M. Environment, "Discovery studio visualizer version 4.0," 2016.

[101] Morris, G. M., Huey, R. Lindstrom, W. Sanner, M. F. Belew, R. K., Goodsell, D. S., Olson, and A. J., "Autodock4 and autodocktools4," 2009.

[102] F. W. L. Immel and S., "No titletop of page solid-state structures of cyclodextrins, cyclodextrin inclusion complexes, and related compounds," 1996. [Online]. Available: http://csi.chemie.tu-darmstadt.de/ak/immel/structures/cyclodextrins/index.html

[103] Steiner, Thomas, Koellner, and Gertraud, "Crystalline .beta.-cyclodextrin hydrate at various humidities: Fast, continuous, and reversible dehydration studied by x-ray diffraction," *Journal of the American Chemical Society*, vol. 116, no. 12, pp. 5122–5128, jun 1994. [Online]. Available: http://pubs.acs.org/doi/abs/10.1021/ja00091a014

[104] K. Harata, C. T. Rao, J. Pitha, K. Fukunaga, and K. Uekama, "Crystal structure of 2-o-[(s)-2-hydroxypropyl]cyclomaltoheptaose." *Carbohydrate research*, vol. 222, pp. 37–45, dec 1991. [Online]. Available: http://www.ncbi.nlm.nih.gov/pubmed/1813110

[105] F. Jensen, "Estimating the Hartree - Fock limit from finite basis set calculations," *Theoretical Chemistry Accounts*, vol. 113, no. 5, pp. 267–273, 2005.

[106] A. Karton and J. M. L. Martin, "Comment on: "Estimating the Hartree-Fock limit from finite basis set calculations" [Jensen F (2005) Theor Chem Acc 113:267]," *Theoretical Chemistry Accounts*, vol. 115, no. 4, pp. 330–333, 2006.

[107] I. D. MacKie and G. A. DiLabio, "Approximations to complete basis set-extrapolated, highly correlated non-covalent interaction energies," *Journal of Chemical Physics*, vol. 135, no. 13, 2011.

[108] S. F. Boys and F. Bernardi, "The calculation of small molecular interactions by the differences of separate total energies. Some procedures with reduced errors," *Molecular Physics*, vol. 19, no. 4, pp. 553–566, 1970.

[109] T. Helgaker, P. Jorgensen, and J. Olsen, *Molecular Electronic-Structure Theory*. Chichester, UK: John Wiley and Sons, Ltd, aug 2000. [Online]. Available: http://doi.wiley.com/10.1002/9781119019572

[110] L. Leclercq, V. Nardello-Rataj, G. Rauwel, and J. M. Aubry, "Structure-activity relationship of cyclodextrin/biocidal double-tailed ammonium surfactant host-guest complexes: Towards a delivery molecular mechanism," *Eur. J. Pharm. Sci.*, vol. 41, no. 2, pp. 265–275, 2010.

[111] B. Komjáti, Á. Urai, S. Hosztafi, J. Kökösi, B. Kováts, J. Nagy, and P. Horváth, "Systematic study on the TD-DFT calculated electronic circular dichroism spectra of chiral aromatic nitro compounds: A comparison of B3LYP and CAM-B3LYP," *Spectrochimica Acta - Part A: Molecular and Biomolecular Spectroscopy*, vol. 155, pp. 95–102, 2016.

[112] W. Klopper and J. Noga, "An explicitly correlated coupled cluster calculation of the helium-helium interatomic potential," *The Journal of Chemical Physics*, vol. 103, no. 14, pp. 6127–6132, 1995.

[113] R. Hoffmann, "Molecular Beauty," *Interdisciplinary Science Reviews*, vol. 16, no. 4, pp. 301–312, dec 1991. [Online]. Available: http://www.tandfonline.com/doi/full/10.1179/isr.1991.16.4.301

[114] J. Graton, B. Legouin, F. Besseau, P. Uriac, J.-Y. Le Questel, P. van de Weghe, and D. Jacquemin, "Molecular Tweezers in Host–Guest Complexes: A Computational Study through a DFT-D Approach," *The Journal of Physical Chemistry C*, vol. 116, no. 43, pp. 23 067–23 074, nov 2012. [Online]. Available: http://pubs.acs.org/doi/10.1021/jp307188q

Biography

Name	Miss Ornin Srihakulung
Date of Birth	25 July 1985
Educational Attainment	Master's degree: Chulalongkorn University, Metallurgy Engineering March, 2014 Bachelor's degree: Chiangmai University, Industrial Engineering March, 2006
Scholarship	2015-2018: JAIST-SIIT-NECTEC Scholarship
Work Experiences	2010-2015: Defence Technology Institute
Publications	O. Srihakulung, L. Lawtrakul, P. Toochinda, W. Kongprawechnon, A. Intarapanich, and R. Maezono, "Theoretical investigation of molecular calculations on inclusion complexes of plumbagin with β-cyclodextrins," in 2017 Fourth Asian Conference on Defence Technology - Japan (ACDT), 2017, pp. 1-5.
	O. Srihakulung, R. Maezono, P. Toochinda, W. Kongprawechnon, A. Intarapanich, and L. Lawtrakul, "Host-Guest Interactions of Plumbagin with β-Cyclodextrin, Dimethyl-β-Cyclodextrin and Hydroxypropyl-β-Cyclodextrin: Semi-Empirical Quantum Mechanical PM6 and PM7 Methods" Sci. Pharm. 2018, 86(2), 20; https://doi.org/10.3390/scipharm86020020